



# **Early Carboniferous lignophyte tree diversity in Australia: Woods from the Drummond and Yarrol basins, Queensland**

Anne-Laure Decombeix, Jean Galtier, Stephen McLoughlin, Brigitte Meyer-Berthaud, Gregory Webb, Paul Blake

## **► To cite this version:**

Anne-Laure Decombeix, Jean Galtier, Stephen McLoughlin, Brigitte Meyer-Berthaud, Gregory Webb, et al.. Early Carboniferous lignophyte tree diversity in Australia: Woods from the Drummond and Yarrol basins, Queensland. *Review of Palaeobotany and Palynology*, 2019, 263, pp.47-64. <10.1016/j.revpalbo.2019.01.009>. <hal-02132903>

**HAL Id: hal-02132903**

**<https://hal.science/hal-02132903v1>**

Submitted on 12 Oct 2021

**HAL** is a multi-disciplinary open access archive for the deposit and dissemination of scientific research documents, whether they are published or not. The documents may come from teaching and research institutions in France or abroad, or from public or private research centers.

L'archive ouverte pluridisciplinaire **HAL**, est destinée au dépôt et à la diffusion de documents scientifiques de niveau recherche, publiés ou non, émanant des établissements d'enseignement et de recherche français ou étrangers, des laboratoires publics ou privés.



HAL Authorization

**Early Carboniferous lignophyte tree diversity in Australia: woods  
from the Drummond and Yarrol basins, Queensland.**

Anne-Laure Decombeix<sup>1, 2, \*</sup>, Jean Galtier<sup>1</sup>, Stephen McLoughlin<sup>3</sup>, Brigitte Meyer-Berthaud<sup>1</sup>,  
Gregory E. Webb<sup>4</sup>, Paul R. Blake<sup>5</sup>.

<sup>1</sup> *AMAP, Univ Montpellier, CNRS, CIRAD, INRA, IRD, Montpellier, France*

<sup>2</sup> *Department of Ecology and Evolutionary Biology, and Natural History Museum and  
Biodiversity Institute, University of Kansas, Lawrence, KS 66045-7534, USA*

<sup>3</sup> *Department of Palaeobiology, Swedish Museum of Natural History, Box 50007, S-104 05  
Stockholm, Sweden*

<sup>4</sup> *School of Earth and Environmental Sciences, The University of Queensland, Brisbane QLD  
4072, Australia*

<sup>5</sup> *Geological Survey of Queensland, Department of Natural Resources, Mines & Energy, PO  
Box 15216, City East, Queensland 4002, Australia.*

\* Corresponding author, e-mail: [anne-laure.decombeix@cirad.fr](mailto:anne-laure.decombeix@cirad.fr)

**Abstract:** Early Carboniferous (Mississippian) permineralised woods from Australia with multiseriate rays have been customarily assigned or compared to the European genus *Pitus*, despite the absence of information on their primary vascular anatomy. In the context of continuing work on the diversity of Late Devonian and Mississippian floras of Gondwana, we studied new silicified woods with secondary xylem similar to that of *Pitus* (multiseriate rays, araucarioid radial pitting) from two sedimentary basins of Queensland, Australia. In the Drummond Basin, three morphotypes of wood of Viséan age can be distinguished based on ray size in tangential section. Although this variation is similar to that observed between the various European species of *Pitus*, information on the primary vascular anatomy of the trees provided by three incomplete specimens excludes an affinity with *Pitus* for at least two taxa. In the Yarrol Basin, two well-preserved late Viséan trunks also have characters similar to *Pitus* but can be distinguished from that genus and other previously described Mississippian trees, in particular by the anatomy of their primary vascular system and departing leaf traces. They are assigned to a new genus, *Ninsaria*. Collectively, the new specimens from Queensland show that wood traditionally referred to ‘*Pitus*’ from Australia actually belongs to several other types of trees that are not known from Europe or North America, indicating probable floristic provincialism between the Northern and Southern hemisphere floras at this time. These new fossils corroborate the existence of a global Mississippian diversification of (pro)gymnosperm trees already noted in Laurussia. They also indicate that the Mississippian floras of Australia were more diverse and complex than traditionally inferred.

**Key-words:** Fossil wood; progymnosperms; gymnosperms; Tournaisian; Viséan; eastern Australia

## 1. Introduction

This study is part of a continuing investigation of the Late Devonian and Early Carboniferous (Mississippian) floristic diversity of Gondwana, and comparison to floras of Laurussia. A significant diversification of ferns s.l. and lignophytes (progymnosperms and seed plants) during the Mississippian is suggested by anatomically preserved axes from Europe and North America (e.g., Galtier and Scott, 1985; Galtier, 1988; Dunn, 2006; Galtier and Meyer-Berthaud, 2006; Taylor et al., 2009). However, their pattern of diversification in other regions of the world remains obscure owing to the paucity of well-documented specimens from this period. For the supercontinent Gondwana, the most recent general synthesis (Anderson et al., 1999) suggested a significant delay in diversification of seed plants and ferns compared to the northern continents. However, recent studies suggest that these plant groups were present in Gondwana earlier than inferred, at least in the palaeotropics (see Prestianni et al., 2015 for a discussion of high-latitude floras). Australia constitutes a key-region in these investigations, with a significant number of Mississippian anatomically preserved ferns and lignophytes discovered recently at localities in the northeastern part of the country (Hueber and Galtier, 2002; Galtier et al., 2007; Decombeix et al., 2011b).

The presence of carbonised or permineralised gymnospermous wood of Mississippian age in Australia has been reported since at least the 19<sup>th</sup> century (e.g., Jack and Etheridge, 1892; Chapman, 1904; Walkom, 1928; Cook and Rozefelds, 2015). Most reported specimens occur in Viséan (Middle Mississippian) formations and have been assigned to *Pitus*, a genus represented in Europe by large trunks as much as 2 m in diameter and interpreted to have seed plant affinities (e.g., Long, 1979; Galtier, 2002). However, the anatomy of the primary vascular system of the Australian stems has not been described to date, and their assignment to *Pitus* is based solely on the occurrence of multiseriate rays in the secondary xylem. Using this character, Walkom (1928) erected the new species *Pitys* (= *Pitus*) *sussmilchii* for

permineralised woods found in coarse-grained sedimentary rocks of the ‘Kuttung Series’ (now Kuttung Formation; Mond, 1973) near Wallaroba, New South Wales (southeastern Australia). This decision was later criticised by Gordon (1935), who emphasised that the anatomical information available in Walkom's specimen was not sufficient to assign it to *Pitus*. Other woods subsequently documented at Viséan localities of New South Wales have, nevertheless, been assigned to *Pitus* sp. (e.g., Gould, 1975; McKelvey and McPhie, 1985; Morris, 1985). In Queensland (northeastern Australia), Mississippian permineralised woods, including complete trunks, also have been reported but without detailed descriptions or study of their affinities. Following two collecting trips in 2005 and 2008, the presence of three morphotaxa of lignophyte trees was documented in Lower Mississippian deposits of the Broken River Province and the Burdekin Basin, in northeastern Queensland (Fig. 1; Decombeix et al., 2011b). Two of these Tournaisian taxa have a wood anatomy very distinct from *Pitus*. They were assigned to the new genus *Dameria* and to *Protopitys*, a putative heterosporous progymnosperm also known from the Mississippian of Europe and North America (Walton, 1957; Galtier and Scott, 1990; Galtier et al., 1998; Falcon-Lang and Galtier, 2010; Decombeix et al., 2015). The third taxon has a wood anatomy similar to that of *Pitus*, with multiseriate rays and araucarioid radial and cross-field pitting. However, it differs significantly in its pattern of leaf trace emission and in its bark anatomy (Decombeix et al., 2011b; Decombeix, 2013) and should be assigned to a new taxon when enough anatomical information is gathered to characterize it.

Here, we describe slightly younger permineralised wood specimens collected in Middle Mississippian (Viséan) deposits of two other basins of eastern Queensland (Fig. 1). These specimens also have secondary xylem anatomy broadly similar to *Pitus*. From the Drummond Basin, three wood morphotypes can be recognised based on ray size in tangential section, a variation similar to that observed between European species of *Pitus*. In the Yarrol Basin, two

trunk fragments with *Pitus*-like anatomy were collected. We show, based on leaf traces, pith and primary xylem anatomy, that these woods differ from *Pitus*, and from all other contemporaneous taxa. We discuss their implications for understanding Mississippian floristic diversity in Australia.

## **2. Material and methods**

### ***2.1. Drummond Basin woods***

The Upper Devonian to Mississippian Drummond Basin in central Queensland contains predominantly terrestrial sedimentary and volcanic rocks (Veevers et al., 1964; Olgers, 1972, Blake et al., 2012, Purdy et al., 2016), deposited in an extensional foreland basin located on the western margin of the New England Orogen (Fig. 1; Johnson and Henderson, 1991; Davis and Henderson, 1996; Henderson et al., 1998). Three depositional cycles can be recognised (Fig. 2). Cycle 1 (Upper Devonian to Mississippian) corresponds to a continental succession deposited close to a volcanic terrane and is essentially composed of lavas, pyroclastic deposits and richly volcanoclastic sedimentary rocks and sinter deposits, locally hosting permineralised plants (Walter et al., 1996, 1998). Cycle 2 (Mississippian) is represented chiefly by fluvial sandstones. Cycle 3 (Mississippian) is again dominated by felsic–intermediate volcanics and volcanogenic sedimentary rocks. The fossil woods described in this paper were collected from the Ducabrook Formation, within cycle 3. The Ducabrook Formation is more than 2 km thick and has been interpreted to represent fluvial and lacustrine deposits (Olgers, 1972), although shallow-marine incursions may have occurred locally (Veevers et al., 1964). The formation is famous for its middle to late Viséan freshwater fauna that includes the remains of sharks, acanthodians, rhizodonts, lungfishes, and the oldest tetrapod body fossil known thus far in Gondwana (e.g., Thulborn et al., 1996; Warren and Turner, 2004). The similarity of this assemblage to contemporaneous vertebrate assemblages from the Euramerican zone

(Thulborn et al., 1996) supports the idea of a continental connection between Laurussia and Gondwana during the Late Devonian and/or Mississippian.

Plant megafossils from the Ducabrook Formation include *Lepidodendron* and *Stigmaria* (Veevers et al., 1964; White, 1964, 1969, 1986), zygopterid fern stems (S. McLoughlin, unpub. data), and woody axes. This paper focuses on eleven wood specimens collected by the Geological Survey of Queensland at a locality about 120 km southwest of Clermont, in the southern Drummond Basin (coordinates 23°51'36"S, 147°2'24"E; Fig. 2) where fossil wood is relatively common. Palynological studies have indicated a middle to late Viséan age for the Ducabrook Formation (Playford, 1978, 1985; Jones, 1996; Jones et al., 2000). However, palynological sampling for these studies was undertaken relatively high in the >2-km-thick Ducabrook Formation. Both the conformably underlying Star of Hope Formation and the Ducabrook Formation are currently interpreted to be Viséan (Jell, 2013). The wood specimens were collected near the base of the formation whereas other studies were carried out near its top, but the exact age of the base of the Ducabrook Formation is very poorly constrained and we thus favour a general Viséan age for the new specimens. The wood fragments, with field numbers DBW1–DBW11, are strongly silicified and have been studied using classical thin-sections and wafers (Hass and Rowe, 1999) prepared at the University of Queensland (and stored in the collections of the Queensland Museum), and at UMR AMAP, Montpellier.

## **2.2. Yarrol Basin trunks**

The Yarrol Basin is a forearc basin formed during the Middle Devonian to early Permian (Cisuralian) on the eastern side of the New England Fold Belt (orogen), which developed along the active convergent margin of eastern Australia at that time (Figs 1, 3). It contains a thick succession of almost exclusively marine deposits (Murray et al., 1987). The lithological succession has been influenced strongly by contemporaneous felsic–intermediate volcanic

activity of varying intensity on the adjacent orogen (Maxwell, 1964). The thick succession of Mississippian marine clastic–volcaniclastic sediments contains sporadic carbonate units, including several coral-sponge-microbial reefs (Simpson et al., 2012).

Two portions of decorticated trunks (field numbers YB1 and YB2) were collected in the northern part of the Yarrol Basin (23°22'45"S, 150°15'24"E) from an un-named unit in the Rockhampton Group in the original group type area (Fleming, 1967). The trunks occurred in poorly exposed calcareous siltstone and sandstone containing corals and bryozoans between the Lion Creek Limestone and a higher, unnamed limestone that is now known to contain coral faunule D corals equivalent to limestone FC5 of Webb (1990) rather than faunule C corals of the Lion Creek Limestone. The higher limestone was originally considered part of the Lion Creek Limestone faulted into its current position (Webb, 1990), but it is now considered a younger limestone beneath the Pennsylvanian–Cisuralian Lorrain Formation (as defined by Murray et al., 2012) (Fig. 3). The Rockhampton Group is Mississippian, and the age of the unit yielding the wood specimens is constrained to the late Viséan based on coral and brachiopod biostratigraphy (i.e., between coral faunules C and D of Webb, 1990) placing it near the boundaries of the *Rhipidomella fortimuscula* and *Marginirugus barringtonensis* brachiopod zones (Roberts et al., 1993) and the *Montognathus carinatus* and *Gnathodus texanus* – *Gn. bilineatus* conodont zones (Jenkins et al., 1993; Denayer and Webb, 2015). YB1 was cut into 13 pieces labelled A to M at the University of Queensland and thin-sections were prepared from all portions. YB2 is 14.5 × 9 cm in diameter and allows observation of a whole trunk in cross-section. New thin-sections (Hass and Rowe, 1999) and acetate peels using HF (Galtier and Phillips, 1999) were also prepared at UMR AMAP, Montpellier on both YB1 A-M and YB2 to provide additional information.

### 2.3. Methods

Images were taken using Sony XCD-U100CR digital cameras attached to an Olympus SZX12 stereomicroscope and to an Olympus BX51 compound microscope. Cropping, rotation, and adjustments of brightness and contrast of the digital images were applied using Photoshop CS5 version 12.0 (Adobe Systems Inc). Cell and tissue dimensions were measured using ImageJ version 1.45 (Rasband, 1997–2016).

All specimens and slides are part of the collections of the Queensland Museum. Field numbers DBW- and YB- are used in this paper; museum registration numbers and fossil locality details are available upon request to the Geosciences Department of the Queensland Museum, Brisbane.

### **3. Woods from the Drummond Basin**

#### ***3.1. Descriptions (Plates I–III)***

All the specimens possess gymnospermous secondary xylem composed of tracheids and multiseriate parenchymatous rays (Plate I). Specimens DBW1–DBW3, DBW5, DBW7–DBW8, DBW10 and DBW11 represent pieces of wood with no primary tissues preserved. DBW6 is a piece of wood containing vascular traces to lateral appendages. DBW4 corresponds to the central part of an axis with a very compressed and poorly preserved stele surrounded by several centimetres of secondary xylem. DBW9 is also the central part of an axis but, in this case, with the pith and innermost secondary xylem preserved.

In the following description, we first document the wood anatomy for all specimens, then focus on those providing additional information (DBW4, 6, and 9).

##### ***3.1.1. Wood anatomy (all specimens) (Plate I; Fig. 4; Table 1)***

191 With the exception of DBW4, DBW6 and DBW9, which represent the central portions of  
192 axes, all specimens correspond to fragments of wood 2–5 cm wide that incorporate parallel  
193 files of tracheids and are thus interpreted as representing the outer parts of large axes.

194 In cross-section, the tracheids are rectangular, more rarely polygonal, with an average  
195 diameter of 40–50  $\mu\text{m}$  between the specimens (maximum observed diameter 75  $\mu\text{m}$ ). All  
196 specimens incorporate changes in tracheid radial diameter that form more or less obvious  
197 growth rings (Plate I, 1, 4, 7). The preservation of the specimens does not, however, permit  
198 accurate measurement of the thickness of those rings, because some portions are considerably  
199 distorted. The best preserved examples are a few millimetres thick (e.g., 4 and 7 mm in  
200 DBW2). The multiseriate rays are long in transverse section, and separate 4–10 rows of  
201 tracheids (Plate I, 1, 4, 7) depending on the specimen and location within a single specimen.

202 In radial longitudinal section, the tracheid walls have 1–4, commonly two, rows of  
203 araucarioid pits that are 6–11  $\mu\text{m}$  in diameter (Plate I, 3, 6, 9). The pit aperture is oval and  
204 oblique. In some sections, the pits cover the entire width of the radial wall (e.g., Plate I, 6),  
205 whereas in others they are more spaced (e.g., Plate I, 3, 9). In those specimens where cross-  
206 field pitting is preserved, it is typically araucarioid, with numerous small crowded pits (arrows  
207 on Plate I, 3, 9). Ray cells are radially elongate, with vertical to oblique end walls, and many  
208 have dark contents.

209 Although the type of radial pitting is similar in all the specimens, it is possible to  
210 distinguish three morphotypes based on ray size in tangential sections (Plate I, 2, 5, 8). A  
211 summary of the ray characteristics is given for the best preserved specimens of each type  
212 (Table 1) and their general aspect is illustrated (Fig. 4). All types show evidence of ray fusion  
213 in tangential longitudinal section.

214 The first morphotype is represented by a single specimen, DBW2. It is characterised by  
215 rays that are 1–3 cells wide (mean: 1.8) and 1–20 (mean: 6.2) cells high in tangential

longitudinal section (Plate I, 2). Ray cells are circular to rectangular in tangential section and have an average size of  $22 \times 31 \mu\text{m}$ . Ray density is 9 rays/ $\text{mm}^2$ .

The second morphotype is the most abundant, represented by specimens DBW3, DBW4, DBW6, DBW7, DBW10 and DBW11. Specimen DBW6, in which the best preservation of wood characters is found, is used to characterise that morphotype. Rays are 1–4 cells wide (mean 2.4) and 1–60 cells high (mean: 21.7) (Plate I, 5). Individual ray cells tend to be rectangular in tangential section and have an average size relatively similar to the previous type,  $18 \times 31 \mu\text{m}$ . Ray density is lower, at 5 rays/ $\text{mm}^2$ .

Finally, the third morphotype, represented by DBW5 and DBW8, is characterised by rays that are 1–8 cells wide (mean 4.5) and 1–25 cells high (mean 11) (Plate I, 8). Ray cells in these specimens are much more circular in tangential section than in the two previous forms, and have average dimensions of  $27 \times 29 \mu\text{m}$ . Ray density is 6.5/ $\text{mm}^2$ .

#### *3.1.2. Compressed axis (DBW4) (Plate II, 1-4; Fig. 5)*

This specimen is an axis  $5.3 \times 4.4 \text{ cm}$  in diameter. The central zone, which corresponds to the pith and primary xylem, is  $1.2 \times 0.3 \text{ cm}$  in cross-section; the oblong shape is probably due to strong compression of the axis (Fig. 5). Cells of the central zone have been replaced by crystals, so the anatomy of the pith and primary xylem remains unknown. However, several small vascular strands and traces to lateral appendages are evident at the periphery of this region (Fig. 5; Plate II, 1–4). Maturation appears to be endarch in most of the strands and in some of the traces as they depart from the stele (Plate II, 1). Further away, the traces have a more mesarch aspect with a small amount of parenchyma on their adaxial side (Plate II, 2). The departing traces are small (slightly less than  $300 \mu\text{m}$  in diameter). The primary xylem tracheids of the traces are up to  $60 \mu\text{m}$  in diameter. Up to nine of these vascular traces are evident on a single transverse section, indicating a compact organotaxis in this part of the

axis, and traces can be followed on successive sections 2 mm apart (Fig. 5). Their arrangement (Fig. 5A), suggests that they may have been produced in groups of three. However, the order of emission of the traces within each group is not obvious. No traces were observed further than 3 mm from the pith, which suggests that the vascularised organs were abscised early in the ontogeny of the axis.

The secondary xylem of the specimen is compressed and it is difficult to assess the presence of growth interruptions. Where they are well-preserved, the secondary xylem tracheids are square to rectangular in transverse section. Their radial walls have 1–3 rows of araucarioid pits with a small aperture. Rays are uni- to triseriate and high in tangential longitudinal section and correspond to those of the second wood morphotype described above.

#### *3.1.3. Wood with vascular traces to lateral appendages (DBW6) (Plate II, 5–6)*

DBW6 is a piece of secondary xylem in which tracheid files tend to be strongly convergent indicating that the centre of the axis was very close to the preserved portion. In its most internal part, the wood contains a group of three small successive vascular traces that are very close to each other (Plate II, 5). Each trace contains a single strand of protoxylem and is accompanied by a very small amount of parenchyma on its abaxial side (Plate II, 6). The wood is of the same type (second morphotype) as the preceding specimen.

#### *3.1.4. Central part of axis (DBW9) (Plate III)*

This small specimen is 2.5 cm in diameter and corresponds to a piece of parenchymatous pith with a small portion of secondary wood preserved on one side (Plate III, 1). In addition to typical parenchyma cells, the pith also contains isodiametric cells with thicker walls that form 0.5–1-mm-wide dark clusters (Plate III, 1–3). Because only the innermost part of the wood (<2 mm) is preserved, ray size is difficult to interpret but rays appear to be uni- to biseriate

and similar to the first or second wood morphotype (Plate III, 4). Limited information on the primary xylem and on a departing leaf trace is available from the small zone preserving the pith–secondary xylem boundary (Plate III, 1, 4, 5). All primary xylem strands appear to be in contact with the secondary xylem, i.e., no medullary or peri-medullary strands are evident (Plate III, 1, 4). The departing trace contains a single mesarch strand of primary xylem (Plate III, 5) and a small strand (not visible on the photo) appears to be lying in a radial to slightly oblique plane from the trace. Because the preservation of the pith–secondary xylem boundary is not only restricted to a small sector of the specimen but also to a very short vertical distance, the whole process of trace emission could not be investigated further.

### **3.2 Affinities**

The new specimens from the Drummond Basin raise two main questions: (1) how many taxa are present? and (2) how do they compare to *Pitus*, the genus to which similar woods have traditionally been assigned in Australia? We will first discuss how the different morphotypes of wood found in the Ducabrook Formation answer these questions, then we will show the significant insights revealed by the specimens with a partly preserved primary vascular system.

#### **3.2.1. Do the different wood morphotypes represent different taxa?**

When the average ray width and height of the three specimens representing the types are compared, T-test (95%) results indicate that DBW6 has significantly higher rays than DBW2 and DBW5, and DBW5 has significantly broader rays than the two other specimens. However, when ray width and height is plotted, it is evident that there is some significant overlap in ray size for the small values between the different types (Fig. 6). Although the wood of the second (DBW6) and third (DBW5) morphotypes can contain respectively higher

and broader rays, it also includes rays of small size, similar to those of the first morphotype. It must be noted that all three morphotypes include at least one specimen with almost parallel files of tracheids, suggesting that they correspond to a relatively mature part of the wood, at considerable distance from the pith.

A similar type of variation in wood anatomy is known to occur in *Pitus*, which represents the best point of comparison despite the fact that the new specimens probably belong to a different genus (see next §). Gordon (1935) differentiated *Pitus* species by the width of their rays (maximum and average size) and the shape of the tracheids (straight or curved). He indicated that “beyond the immediate neighbourhood of the medulla” the rays in all species were relatively constant in width. Ray height in *Pitus* wood has also been observed at various distances from the pith in a trunk of *P. withami* from the Viséan of Scotland (Galtier and Scott, 1994). Although the maximum height increases toward the periphery of the trunk, the average ray height remains the same and was thus identified as a potentially useful taxonomic character within the genus. More recently, Henderson and Falcon-Lang (2011) conducted a principal component analysis on 34 Early Mississippian specimens of *Pitus* from Scotland to separate phylogenetic from ontogenetic variations in wood anatomy. The analysis included not only characters of the rays, such as height and width, cell dimension, and ray density, but also tracheid diameter and the number of rows of radial pits. It revealed the presence of six distinct wood morphotypes, which were interpreted by the authors as representing at least three biological taxa. On the basis of these previous works on *Pitus*, it seems questionable to consider that the three wood morphotypes from the Ducabrook Formation are simply ontogenetic variants of a single taxon, especially given the lack of information on the primary vascular anatomy corresponding to each type of wood. Thus, we propose that the three wood morphotypes be interpreted as evidence of the presence of three taxa.

### 3.2.2. *Mississippian taxa with similar types of wood (Table 2)*

Several Mississippian taxa from Europe, North America, North Africa, and Australia have secondary xylem generally similar to the Drummond Basin specimens, with araucarian radial pitting, araucarioid cross-field pitting, and multiseriate parenchymatous rays. Isolated pieces of wood with this anatomy are assigned by some workers to the morphogenus *Dadoxylon* Endlicher—in contrast to similar woods with only uniseriate rays, which are assigned to *Agathoxylon* Hartig (= *Araucarioxylon*, see Rößler et al., 2014). At least eight Mississippian genera of stems with this type of wood anatomy have been recognised to date: *Ahnetia* (Decombeix and Galtier, 2017), *Archaeopitys* (Scott and Jeffrey, 1914), *Cauloxylon* (Cribbs, 1939), *Eristophyton* (Scott, 1902; Lacey, 1953; Galtier and Scott, 1990; Decombeix et al., 2007, 2008), *Faironia* (Decombeix et al., 2006), *Megalomyelon* (Cribbs, 1940), *Picnoxylon* (Cribbs, 1938) and *Pitus* (Gordon, 1935). Ray size in these taxa and in isolated pieces of wood, such as ‘*Dadoxylon*’ *ambiguum* and *Paleoxylon bourbachensis*, were compared to those of the specimens from the Ducabrook Formation (Table 2). DBW2, which has the lowest and narrowest rays, is most similar to the secondary xylem of *Eristophyton fasciculare* and of *Dadoxylon ambiguum* (Scott, 1902; Galtier and Scott, 1990; Galtier et al., 1998). DBW6, representing the most abundant morphotype among the Ducabrook specimens, is most similar to *Paleoxylon bourbachensis*. This species has been compared to *Pitus withami* by Galtier et al. (1998) but on average its rays are slightly taller and broader. Finally, DBW5 and DBW8, characterised by very wide rays, are most similar to the wood of *Pitus dayi* (Gordon, 1935). The only taxon with wood similar to some of the Drummond Basin specimens described in detail from Australia (MSM11) has a ray size similar to specimens of the DBW6 type (Decombeix et al., 2011b, see also below).

### 3.2.3. *Importance of the specimens preserving vascular traces to lateral appendages*

Specimens DBW4, DBW6, and DBW9 are the only specimens providing information on the primary structure of some of the lignophyte trees preserved in the Ducabrook Formation. How do their features compare to those of previously described Mississippian arborescent lignophytes?

The primary vascular structure of DBW4 is characterised by a stele with numerous, small, endarch to mesarch primary xylem strands and departing leaf traces. Because the pith is not preserved, it is not possible to exclude the presence of medullary and/or peri-medullary primary vascular strands. There is also no way to document with certainty the presence of reparatory stands near or facing the departing traces. However, the endarch maturation of some visible strands and departing leaf traces is a notable difference from several arborescent Mississippian genera, including *Pitus* (Scott, 1902; Gordon, 1935; Long, 1979), *Archaeopitys* (Scott and Jeffrey, 2014), *Megalomyelon* (Cribbs, 1940) and *Faironia* (Decombeix et al., 2006), which all have a strictly mesarch maturation. Two other European genera, *Eristophyton* and *Bilignea*, have a maturation that changes from endarch to mesarch at the nodes (Scott, 1924; Decombeix et al., 2007 and references therein); a similar pattern apparently occurs in *Pycnoxylon* from the Tournaisian of Missouri (Cribbs, 1938). This does not seem to be the case in the Australian specimen (DBW4). In *Ahnetia* from the Tournaisian of Algeria (Decombeix and Galtier, 2017), maturation in the largest strands is mesarch, whereas the smallest strands consist only of a few tracheids and maturation is difficult to assess. Genera that have a strictly endarch maturation include *Endoxylon* (Scott, 1924; Lacey, 1953) and *Cauloxylon* (Cribbs, 1939). *Endoxylon* can be distinguished from DBW4 by the stele containing only a few large primary xylem strands. In *Cauloxylon*, primary xylem strands are typically in a peri-medullary position, separated from the wood by several layers of parenchyma. However, we should consider that such strands may not have been preserved in DBW4 and that only strands departing as traces are visible. In *Cauloxylon*, however, the

departing trace very quickly shows two radially aligned poles of protoxylem, which distinguish this genus from DBW 4, in which only one pole is evident.

Sections of DBW4 show, at the same vertical level, groups of closely spaced vascular traces departing to lateral organs (Fig. 5). Superficially, this might suggest an artefact due to compression of the axis and might be a deformation of the central part. However, that this pattern might relate to the true organotaxis is supported by the existence of two other specimens showing a similar organisation, one from the same locality (DBW6) and one described previously from Lower Mississippian strata of the nearby Burdekin Basin (Decombeix et al., 2011b; see Fig 1). These two specimens have a secondary xylem anatomy similar to that of DBW4. DBW6 is a wood fragment that, in its most internal part, has a group of three small vascular traces that are very closely spaced (Plate II, 5). The secondary xylem surrounding these traces shows no significant deformation and there is no doubt that the close arrangement of the traces is not an artefact. This supports the contention that groups of traces are emitted in some of the woody plants from the Ducabrook Formation. The specimen from the Burdekin Basin (MSM11 of Decombeix et al., 2011b) has a preservation similar to DBW 6, i.e., its central part is present but not preserved. It also shows the emission of closely located traces at some levels and its secondary xylem anatomy is similar to that of DBW4 (see Table 2). Based on this evidence, two hypotheses need to be considered: (1) that these plants had a complex organotaxis with multiple spirals, or (2) that several vascular traces supplied a single lateral organ. The vascularisation of a single lateral organ by multiple traces is documented in several Mississippian (pro)gymnosperm taxa. The non-arborescent calamopityalean seed ferns *Diichnia* (Beck et al., 1992) and *Triichnia* (Galtier and Beck, 1992), respectively, have double and triple vascular traces to their leaves. Similarly, *Faironia*, which has characters of both arborescent (e.g., *Pitrus*) and non-arborescent (e.g., Calamopityales) Mississippian taxa, produced pairs of traces that divided and vascularised a

single petiole in the cortex (Decombeix et al., 2006). *Cauloxylon*, *Picnoxylon* and *Megalomyelon*, three (pro)gymnosperms trees from the Early Mississippian of Missouri, also have vascular traces apparently emitted in pairs (Cribbs, 1938, 1939, 1940). Because these traces were rapidly occluded in the wood of the trunks, it is uncertain whether they vascularised a single organ. With the exception of the calamopityean *Triichnia*, which has a very different wood from the Ducabrook Formation specimens (Galtier and Beck, 1992), *Megalomyelon* is the only taxon in which some groups contain more than two traces (Cribbs, 1940). However, it differs from the Australian specimens by its mesarch maturation and its mostly uniseriate to partly biseriate rays. Thus, the information available from DBW4 and DBW6 does not allow their confident assignment to any previously described taxon of Mississippian (pro)gymnosperm.

The third specimen providing information on the primary vascular structure of the trees from the Ducabrook Formation is DBW9. The lack of immersed strands either in the medullary or peri-medullary regions of its pith rules out an affinity with *Ahnetia*, *Archaeopitys*, *Cauloxylon*, *Eristophyton waltonii*, *Faironia*, *Megalomyelon*, *Picnoxylon* or *Pitus* (Scott and Jeffrey, 1914; Cribbs, 1939, 1939, 1940; Lacey, 1953; Decombeix et al., 2006; Decombeix and Galtier, 2017). The lack of tracheids in the pith also distinguishes it from *Bilignea* (Scott, 1924). Moreover, the small size of the primary xylem strands distinguishes it from *Endoxylon* and from *Eristophyton fasciculare*, *E. beneirtianum* and *E. feisti*. Such very small strands occur in *E. waltonii* and *Ahnetia* but, as mentioned above, other characters including the location of the strands rule out any affinity with these taxa. Thus, the information available on the primary vascular anatomy indicates that DBW9, like DBW4 and DBW6, is both distinct from *Pitus* and not assignable with confidence at this stage to any other previously described Mississippian lignophyte genus.

### 3.2.4. Summary

Woods from the base of the Ducabrook Formation in the Drummond Basin can be assigned to three morphotypes based on ray size. Some information on the primary vascular structure is available for one of these morphotypes and possibly a second. No primary vascular information is available for the morphotype with very broad rays. The specimens have a secondary xylem anatomy similar to that of some coeval arborescent lignophytes reported previously from Europe and North America, such as *Eristophyton* and *Pitus*, but the information available on their primary anatomy does not permit their assignment to established species. At this stage, we do not formalise new taxa for the woody plants from the Ducabrook Formation, because we consider that additional axes with more anatomical characters preserved are required to fully circumscribe their features.

## 4. Trunks from the Yarrol Basin

### 4.1. Descriptions

The two available specimens appear similar for all observed characters and are thus described together. In cross-section, the centre of the trunks is composed of a broad parenchymatous pith (Fig. 7) with numerous small primary xylem strands distributed in a peri-medullary position. The preserved secondary xylem is up to 5.5 cm thick. Tissues centrifugal to the secondary xylem are not preserved.

#### 4.1.1. Pith (Plate IV; Fig. 7)

The pith is elliptical, about 30 × 25 mm in YB1 and 35 × 25 mm in YB2, and its tissues are extremely well-preserved. It is composed of parenchymatous cells, some with a conspicuous dark content (Plate IV, 1, 2). The parenchyma cells are polygonal, with an average diameter of 151 µm (84–229 µm). Most are slightly elongate radially except in the center of the pith

where they are isodiametric. The cells with dark content are distributed randomly within the pith and represent about 1/25 of the pith cells. In some cases, the content appears as a reticulum slightly detached from the cell walls (Plate IV, 2). Many of the dark cells show evidence of derivation from a common mother cell and occur in pairs (Plate IV, 2). The divisions appear to occur variably in the radial or tangential plane.

#### *4.1.2. Primary vascular anatomy and vascular traces to lateral organs (Plate IV, V; Fig. 7, 8)*

The contact zone between the pith and the secondary xylem is not preserved throughout the circumference of the specimens (e.g., Fig. 7; Plate IV, 1) so the complete architecture of the primary vascular system could not be reconstructed. However, observations of the best preserved parts of YB1 and YB2 provide valuable information on the primary xylem and departing leaf traces. Primary xylem strands form a ring in the outermost part of the pith (Fig. 8; Plate IV, 3). About 35–40 strands are distributed around the circumference of the pith in YB1. Given the existence of non-preserved zones, the original number is estimated to be closer to 50. Primary xylem strands are positioned 1–2 mm apart (Fig. 8; Plate IV, 3). Their size and shape are highly variable, as is their distance to the secondary xylem and to adjacent strands (Fig. 8; Plate IV, 3–5). This variability is probably due to significant changes in strand size, location, and number in the zones of incipient leaf trace emission. The smallest strands are composed of a few tracheids and are about 100 µm wide or less. They are typically separated from the secondary xylem by 5–7 parenchyma cells (Plate IV, 3, 4). The largest strands are about 200 µm in diameter (Plate IV, 5, 6). There is some evidence of strand division. Some primary xylem strands have 1–3 tracheids of smaller diameter interpreted as protoxylem tracheids, and the maturation in most cases appears to be endarch (Plate IV, 4), although some of the largest strands have a more mesarch appearance. In other strands, it is impossible to clearly identify the protoxylem.

Several vascular traces departing to lateral organs are evident in the peels and thin-sections (Plate IV, 5; Plate V; Fig. 7; Fig. 8). A general view of the trunk YB2 shows two relatively close traces in the wood (Fig. 7, arrows top left). Two other, much less advanced, departing traces are visible in the right part of the specimen and form a 140° angle with the previous two. The distance between two traces of a pair is about 5 mm and a closer examination shows that one of the two traces is slightly more advanced than the other. The other regions of the pith-secondary xylem boundary are not well preserved; thus, it is impossible to follow leaf trace emission on that specimen. Investigation of YB1 provides crucial additional information. Several leaf traces at different stages of emission can be seen on a given cross-section. They are usually 4–6 mm apart and separated by a few very small strands composed of a few tracheids (Fig. 8). The occurrence of pairs of traces noted on YB2 is supported by the presence of ‘successive’ traces at a relatively similar stage of emission (T1, T2 in Fig. 8B). However, it is not entirely certain that this is a consistent pattern owing to the incompleteness of the primary xylem zone around the circumference of the pith in both specimens.

Although some features are not entirely clear, general stages of leaf trace emission can be recognised from the observation of several sections. The first recognizable stage of leaf trace production is the enlargement and division of an immersed primary xylem strand. This leads to the formation of a larger, broadly triangular strand that moves closer to the secondary xylem (Fig. 8; Plate V, 1). Files of secondary xylem tracheids take on a curved aspect where the leaf trace is going to be emitted. At a more advanced stage, the strand divides radially and a complex of primary xylem strands is formed in the zone facing the location of the leaf trace departure (Fig. 8; Plate V, 2, 3, 5, 6, red arrowheads). There is a conspicuous neighbour strand about 100 µm wide orientated slightly obliquely about 1 mm from the trace (Fig. 8; Plate V, 1, 2, 3, yellow arrowheads). A group of a few tracheids is also present on the other side of the incipient leaf trace but it is much less conspicuous and not visible in all cases (Fig. 8; Plate V,

3). At an even more advanced stage, the departing leaf trace contains three radially aligned protoxylem strands protruding through the secondary xylem (Fig. 8; Plate IV, 5; Plate V, 4, 7). The trace is then about  $1.2 \times 0.5$  mm in major dimensions, much larger than the largest primary xylem strands (Plate IV, 5; Plate V, 4). As the leaf trace departs, the neighbor strand moves a little more to the side but remains clearly present, and the small strands of primary xylem composed of a few tracheids that were facing the trace (Plate V, 2, 5) apparently disappear (Plate V, 4). Although a lateral strand located about 1 mm from the site of the leaf trace emission is a constant feature in all departing traces that we observed, its origin and relation to the leaf trace remains uncertain. It is present in the earliest stages of leaf trace emission and it is unclear whether it (1) results from a division of the large strand that gives off the trace (reparatory strand), (2) results from the increase in size of a previously non-detected strand composed of a few tracheids, or (3) arises *de novo*.

#### 4.1.3. Secondary xylem (Plate VI)

The secondary xylem consists of tracheids and multiseriate parenchymatous rays (Plate VI, 1–3). In cross-section, the wood shows some growth ring boundaries (Plate VI, 3). The best preserved rings are 3–7 mm in width. False rings, characterised by 3–5 rows of tracheids with a reduced radial diameter, are also present sporadically. The secondary xylem tracheids are polygonal in cross-section and 17–75  $\mu$ m in diameter. The rays are long; some cross the entire wood cylinder. They separate 2–10 files of tracheids and are expanded in the pith region by enlargement of the cells (Plate VI, 1–3).

Tracheids are not pitted on their tangential walls. The rays are 2–5 cells wide in tangential section and up to 60 cells high (Plate VI, 4–5). The average size for 100 measured rays is 2.7 cells wide and 14 cells high. Ray cells are circular to polygonal in tangential longitudinal section, with variable sizes. They are 32 (16–53)  $\mu$ m wide and 55 (30–79)  $\mu$ m high.

In radial longitudinal section, tracheid walls bear 1–4 rows of pits that are hexagonal to circular (Plate VI, 6–7). The pits cover the entire width of the radial walls. Almost 80% of tracheids have two or three rows of pits, which are always arranged alternately. They measure 14  $\mu\text{m}$  (10–20  $\mu\text{m}$ ,  $n=30$ ) in diameter and have an oblique, slit-like to oval aperture (Plate VI, 7). Ray cells are 81–257  $\mu\text{m}$  long with vertical walls. There are no ray tracheids. Cross-fields bear araucarioid pitting, with 6–12 crowded oval to circular pits (Plate VI, 8).

#### 4.2. Affinities

The Yarrol Basin trunks are characterised by (1) a large parenchymatous pith, (2) numerous small primary xylem strands in a peri-medullary position, (3) leaf traces probably emitted in pairs, much larger than the primary xylem strands, and containing three radially aligned protoxylem strands as they depart from the stele, and (4) secondary wood with multiseriate rays, araucarian radial pitting and araucarioid cross-field pitting. *Ahnetia* (Decombeix and Galtier, 2017), *Archaeopitys* (Scott and Jeffrey, 1914), *Cauloxylon* (Cribbs, 1939), *Eristophyton waltonii* (Lacey, 1953; Galtier and Scott, 1990), *Faironia* (Decombeix et al., 2006), *Megalomyelon* (Cribbs, 1940), *Picnoxylon* (Cribbs, 1938) and *Pitus* (Gordon, 1935) share with the new trunks the presence of a parenchymatous eustele with numerous small primary xylem strands in a peri-medullary position. Two main characters distinguishing the Australian trunks from *Archaeopitys*, *Faironia*, *Megalomyelon* and *Pitus* are the presence of endarch maturation in most strands and the presence of several radially aligned strands in the departing vascular trace to lateral appendages. An additional difference from *Archaeopitys* and *Pitus* is the lack of true medullary strands in the Australian trunks; however, although this condition has been recorded in all species of *Pitus*, it is not necessarily represented in all specimens of that genus (Gordon, 1935). Both *Picnoxylon* and *Eristophyton waltonii* have a maturation that changes from endarch between nodes to mesarch at the nodes (Cribbs, 1938;

Lacey, 1953). Although this is more similar to the maturation in the Yarrol Basin trunks, the latter can again be distinguished by their more complex leaf traces.

*Ahnetia* from the Mississippian of Algeria (Decombeix and Galtier, 2017) has some similarities with the specimens from the Yarrol Basin, including the presence of small perimedullary primary xylem strands, a complex production of leaf traces, and a wood with rays that are 1–5 cells wide and 1–50 cells high. On the other hand, *Ahnetia* differs significantly from the new specimens by the greater distance between strands (about 6 mm), and its smaller leaf traces with a single protoxylem strand. There is also no evidence of pairs of traces in *Ahnetia*. It is notable, however, that the stages of primary xylem strand changes leading to leaf trace production in *Ahnetia* are quite similar to those of the new specimens, including the formation of a large triangular primary xylem strand with several protoxylem poles and the presence of a conspicuous lateral strand, whose origin in *Ahnetia* remains unclear.

Finally, *Cauloxylon* from the late Tournaisian of Missouri (Cribbs, 1939) shares some important characters with the new specimens, including much reduced primary xylem strands (2–4 tracheids in some cases), endarch maturation even in some large strands, complex branching of strands prior to leaf trace departure, the occurrence of paired traces separated by a few small strands, and the presence of more than one protoxylem strand in the departing trace. The secondary xylem of *Cauloxylon* is also broadly similar to that of the Australian trunks, but the rays are a larger (1–7) and taller (commonly 30–40 cells tall versus an average of 14 for the Australian trunks). However, *Cauloxylon* also differs from the Australian trunks by several characters, including the presence of sclerotic nests in the pith, the presence of two radially aligned poles of protoxylem in the departing trace, versus three in the Australian trunks, and smaller traces (200–400  $\mu\text{m}$ ).

Although the new trunks from the Yarrol Basin share several significant characters with arborescent lignophytes from Europe, North America and North Africa they do not appear to

fit the diagnosis of any genus described previously. They might, however, belong to a group of Mississippian trees with a complex primary vascular architecture that includes taxa such as *Cauloxylon* or *Ahnetia* from the late Tournaisian of USA and Algeria, respectively. It is interesting to note that this type of complex primary vascular organisation has not been described previously in Viséan taxa.

It should be noted that although Carboniferous woody axes with a preserved pith and primary vascular system have been reported in South America, they are younger than the other taxa mentioned here (Late Mississippian or Pennsylvanian) and typically comprise wood with uniseriate rays and a much more simple organization of the primary xylem and leaf traces (e.g., Pujana, 2005; Pujana and Césari, 2008).

Cells with marginally contracted dark contents (Plate IV, 2), commonly in the form of a three-dimensional filamentous reticulum, have been noted from a diverse range of woods and rhizomes of Carboniferous to Cretaceous age in several earlier studies (e.g., Andrews and Lenz, 1943; Smoot and Taylor, 1983; Tidwell and Herbert, 1992; Weaver et al., 1997; Strullu-Derrien et al., 2012; McLoughlin and Strullu, 2016; Krings et al., 2017). Their filamentous character is reminiscent of fungal hyphae, but they may alternatively represent biomimetic mineral precipitates (Klymiuk et al., 2013), some of which may have been mediated by various bacterial groups during early diagenesis (Konhauser, 1997; Baumgartner et al., 2006; Krings et al., 2017). They appear to have no significance for systematic placement of the Yarrol Basin woods.

#### **4.3. Systematic palaeobotany**

Unranked clade: Lignophytia Kenrick and Crane 1997.

Class, order and family: Incertae sedis.

***Ninsaria* Decombeix, Galtier, McLoughlin, Meyer-Berthaud gen. nov.**

591 *Type species: Ninsaria australiana* Decombeix, Galtier, McLoughlin, Meyer-Berthaud sp.  
592 nov. (here designated).

593 *Generic diagnosis:* Stem with primary and secondary vascular tissues. Eustele consisting of  
594 numerous small discrete strands of primary xylem at the periphery of a broad parenchymatous  
595 pith. Primary xylem strands in peri-medullar position, composed of a few tracheids. Leaf trace  
596 emission starting with two divisions of a primary xylem strand and formation of an arc-  
597 shaped group of three strands that progresses towards the secondary xylem. Departing leaf  
598 trace much larger than axial strands, with three radially aligned protoxylem strands. Leaves  
599 arranged in a complex spiral. Secondary xylem tracheids with multiseriate araucarioid  
600 bordered pits on radial walls. Cross-field pitting araucarioid. Rays multiseriate, of medium  
601 height.

602 *Etymology:* After Ninsar, the Sumerian goddess of plants.

603 ***Ninsaria australiana* Decombeix, Galtier, McLoughlin, Meyer-Berthaud sp. nov**

604 *Holotype:* YB1, Plates IV, V (2–7), VI.

605 *Paratype:* YB2, Plate V(1).

606 *Stratigraphic and geographic occurrence:* Unnamed bed within the Rockhampton Group  
607 between the Lion Creek Limestone and Lorrain Formation; from exposures between localities  
608 UQL4887 and UQL4981 of Webb (1990).

609 *Age:* late Viséan.

610 *Etymology:* After Australia, reflecting the geographic origin of the specimens.

611 *Specific diagnosis:* Stem with a 20–30 mm wide eustele, composed of 40–50 axial strands and  
612 incipient leaf traces. Pith of polygonal parenchyma cells, some with dark reticulate content.  
613 Primary xylem strands peri-medullar, separated from the secondary xylem by several layers of  
614 parenchyma cells. Distance between strands 1–2 mm. Primary xylem strands small, typically  
615 <200 µm in diameter, and usually consisting of a few tracheids. Xylem maturation endarch in

small strands. Leaf trace about  $1.2 \times 0.5$  mm. Tracheids of secondary xylem rectangular to polygonal, with average diameter equal to, or slightly larger than, the metaxylem tracheids. Rays up to five cells wide, up to 60 cells in height.

## **5. (Pro)gymnosperm trees in the Mississippian of Australia**

The present work has shown that several taxa with *Pitus*-like wood, i.e., with araucarian pitting and multiseriate rays, are present in Mississippian deposits of Australia. Specimens from the Viséan of the Drummond Basin, like middle Tournaisian specimens reported previously from the Burdekin Basin (Decombeix et al., 2011b) differ from *Pitus* at least by their phyllotaxis. Trunks from the Yarrol Basin also differ from *Pitus*, in this case by several characters of their primary vascular architecture and leaf trace anatomy. All these new specimens appear to be different from previously described species of Mississippian lignophytes. In summary, these examples of taxa with ‘*Pitus*-like wood’ from Australia: (1) are actually distinct from *Pitus*; (2) correspond to more than one taxon; and (3) differ in characters of their primary vascular organisation from Mississippian taxa with a similar wood anatomy currently known from Europe, North America and North Africa (Galtier and Meyer-Berthaud, 2006). These results do not imply the absence of *Pitus* in the Mississippian of Australia, because other specimens with a similar type of wood have been reported for which the anatomy of the primary vascular system remains unknown. However, the specimens from the Drummond and Yarrol basins reveal that the taxonomic diversity of trees with this general type of wood in Australia is higher than initially suspected. This diversity supports previous observations that eastern Australia saw a change in lignophyte tree diversity around the Devonian–Carboniferous boundary similar to that recorded in Laurussia, with the extinction of the arborescent progymnosperm *Archaeopteris* that dominated Late Devonian forests and

the diversification of new taxa of (pro)gymnosperm trees during the Early and Middle Mississippian (Decombeix et al., 2011a).

The occurrence of at least one arborescent species, the progymnosperm *Protopitys* both in Australia and Europe during the middle Tournaisian (Decombeix et al., 2011b, 2015) provides palaeontological evidence of floristic exchange between Gondwana and Laurussia around the Devonian–Mississippian transition. Anatomically preserved plants of smaller size from the locality of Ruxton (northeastern Queensland) also reveal some similarities at least at the generic level between Australian and European taxa (Galtier et al., 2007). There are, however, also several examples of Tournaisian plant genera known only from Australia, such as the arborescent zygopterid fern *Symplocopteris* (Hueber and Galtier, 2002) and the ovulate organ *Ruxtonia* (Galtier et al., 2007). For the Viséan, the trees with *Pitus*-like wood from the Drummond and Yarrol basins represent new examples of plants that are presently documented only in Australia. In this context, it is interesting to note that eastern Australia saw a change from more cosmopolitan conodonts in the Tournaisian to more endemic conodonts in the Viséan, whereas the Viséan corals are clearly endemic; other Viséan marine taxa are, however, considered more cosmopolitan (e.g., Jones et al., 2000; Webb, 2000; Denayer and Webb, 2015)

Morris (1985) considered that, during the Viséan, *Pitus*-like trees formed ombrophile forests with a tree-fern understorey and that this indicated a more humid climate in eastern Australia than during the Tournaisian. This interpretation was based on (1) the association of “*Pitus*” and the zygopteridalean tree-fern *Austroclepsis australis* (Sahni, 1932) in the Viséan of New South Wales, and (2) the fact that tree rings in known specimens of ‘*Pitus*’ were either indistinct or completely absent. The co-occurrence of lignophyte trees with a *Pitus* type of wood and zygopteridalean tree ferns has now also been documented in the middle Tournaisian locality of Dotswood in the Burdekin Basin (Hueber and Galtier, 2002;

Decombeix et al., 2011b) and these ferns are also present in the Drummond Basin (S. McLoughlin, unpub. data). This association can thus be found earlier than the Viséan and is not typical of that age, although the respective taxa of ferns and lignophyte trees might differ between assemblages. No arborescent fern (Zygopteridales or other) is known in the Mississippian of Laurussia, so this association appears to be distinctive to eastern Australia.

Regarding growth parameters, woods from both the Ducabrook Formation (Viséan) and the Yarrol Basin (late Viséan) have distinct growth ring boundaries, which implies that their growth was seasonal. This is particularly interesting when compared to the older specimens from the middle Tournaisian of the Burdekin Basin in which growth rings are much more subtle (Decombeix et al., 2011b; Laloux, unpub. data). This difference could be due to the combined effect of (1) the southward movement of Australia during the Mississippian from tropical to temperate latitudes, and (2) the onset of the Late Paleozoic Ice Age in western Gondwana during the Viséan (e.g., Caputo et al., 2008; Gulbranson et al., 2010). However, only small portions of wood are known from the Drummond and Yarrol basins and, in some cases, they represent the inner part of the trunk, a region for which growth ring anatomy might reflect developmental processes in addition to cambial reaction to environmental constraints. Thus, it is difficult to analyze the possible climatic information provided by those rings in more detail. A warm Viséan interval in Australia has been suggested based on several proxies including compression/impression floras (Iannuzzi & Pfefferkorn, 2002) and reef history (Webb, 2002). The apparently more seasonal growth of the Viséan trees compared to the Tournaisian ones might thus also be linked to a different biology and/or to a different habitat of origin, as the trunks are not found in situ.

## **6. Conclusions**

New permineralised plants with a *Pitus* type of wood are described from the Drummond and Yarrol basins of Queensland, Australia. The woods represent several distinct morphotaxa and the available information on their primary vascular system indicates that they differ from *Pitus* and from other previously described taxa of Mississippian lignophytes. These new specimens increase the known diversity of woody plants in Australia during the Mississippian and show that the floras of the region at this time were more complex than is usually interpreted based on compression/impression specimens.

## Acknowledgements

We thank Pam Wilson and Kristin Spring (Queensland Museum) for their help with the loan. ALD and BMB acknowledge funding from LabEx CeMEB (Exploratory Project MARCON) during the course of this research. Financial support to Stephen McLoughlin by the Swedish Research Council (VR grant 2014-5234) and National Science Foundation (project #1636625) is gratefully acknowledged. AMAP (Botany and Computational Plant Architecture) is a joint research unit which associates CIRAD (UMR51), CNRS (UMR5120), INRA (UMR931), IRD (R123), and Montpellier University (UM); <http://amap.cirad.fr>

## References

- Anderson, J.M., Anderson, H.M., Archangelsky, S., Bamford, M.K., Chandra, S., Dettmann, M., Hill, R., McLoughlin, S., Rösler, O., 1999. Patterns of Gondwana plant colonisation and diversification. *J. Afr. Earth Sci.* 28, 145–167.
- Andrews, H.N., Lenz, L.W., 1943. A mycorrhizome from the Carboniferous of Illinois. *Bull. Torrey Bot. Club* 70, 120–125.

- 712 Baumgartner, L.K., Reid, R.P., Dupraz, C., Decho, A.W., Buckley, D.H., Spear, J.R.,  
 713 Przekop, K.M., Visscher, P.T., 2006. Sulphate reducing bacteria in microbial mats:  
 714 Changing paradigms, new discoveries. *Sediment. Geol.* 185, 131–145.
- 715 Blake, P.R., Withnall, I.W., Fitzell, M.J., Kyriazis, Z., Purdy, D.J., 2012. Geology of the  
 716 western part of the Drummond Basin. *Queensland Geological Record* 2012/17
- 717 Beck, C.B., Galtier, J., Stein, W.E. Jr., 1992. A reinvestigation of *Diichnia* Read from the  
 718 New Albany Shale of Kentucky. *Rev. Palaeobot. Palynol.* 75, 1–32.
- 719 Caputo, M.V., de Melo, J.H.G., Streel, M., Isbell, J.L., 2008. Late Devonian and Early  
 720 Carboniferous glacial records in South America. In: Fielding, C.R., Frank, T.D., Isbell,  
 721 J.L. (Eds.), *Resolving the Late Paleozoic Ice Age in Time and Space*, Geological  
 722 Society of America, Boulder, CO, pp. 161–174.
- 723 Chapman, F., 1904. On a collection of upper Palaeozoic and Mesozoic fossils from Western  
 724 Australia and Queensland, in the National Museum, Melbourne. *Proc. R. Soc. Victoria*,  
 725 N.S., 16, 306–335.
- 726 Cook, A., Rozefelds, A., 2015. *In Search of Ancient Queensland*. Queensland Museum,  
 727 Brisbane, 277 pp.
- 728 Cribbs, J.E., 1938. A new fossil plant from the Reed Spring Formation of southwestern  
 729 Missouri. *Am. J. Bot.* 25, 311–321.
- 730 Cribbs, J.E., 1939. *Cauloxylon ambiguum*, gen. et sp. nov., a new fossil plant from the Reed  
 731 Spring Formation of southwestern Missouri. *Am. J. Bot.* 26, 440–449.
- 732 Cribbs, J.E., 1940. Structure of fossil stem of pityean affinity from the Reed Springs  
 733 Formation of Missouri. *Bot. Gaz.* 101, 582–597.
- 734 Davis, B.K., Henderson, R.A., 1996. Rift-phase extensional fabrics of the back-arc  
 735 Drummond Basin, eastern Australia. *Basin Res.* 8, 371–381

736 Decombeix, A.-L., 2013. Bark anatomy of an Early Carboniferous tree from Australia. IAWA  
737 J. 34, 183–196.

738 Decombeix, A.-L., Galtier, J., 2017. *Ahnetia*, a new lignophyte stem from the Lower  
739 Carboniferous of southern Algeria. Rev. Palaeobot. Palynol. 237, 62–74.

740 Decombeix, A.-L., Galtier, J., Meyer-Berthaud, B., 2006. *Faironia difasciculata*, a new  
741 gymnosperm from the Early Carboniferous (Mississippian) of Montagne Noire, France.  
742 Rev. Palaeobot. Palynol. 142, 79–92.

743 Decombeix, A.-L., Meyer-Berthaud, B., Galtier, J., 2007. A review of the genus *Eristophyton*,  
744 with special focus on the Mississippian species. C. R. Palevol 6, 393–401.

745 Decombeix, A.-L., Meyer-Berthaud, B., Galtier, J., 2008. Diversity of Mississippian  
746 arborescent lignophytes: a new species of *Eristophyton* from the middle Tournaisian of  
747 France. Int. J. Plant Sci. 169, 1116–1127.

748 Decombeix, A.-L., Meyer-Berthaud, B., Galtier, J., 2011a. Transitional changes in  
749 arborescent lignophytes at the Devonian–Carboniferous boundary. J. Geol. Soc. London  
750 168, 547–557.

751 Decombeix, A.-L., Meyer-Berthaud, B., Galtier, J., Talent, J.A., Mawson, R., 2011b.  
752 Arborescent lignophytes in the Tournaisian vegetation of Queensland (Australia):  
753 Palaeoecological and palaeogeographical significance. Palaeogeogr. Palaeoclimatol.  
754 Palaeoecol. 301, 39–55.

755 Decombeix, A.-L., Galtier, J., Prestianni, C., 2015. The Early Carboniferous progymnosperm  
756 *Protopitys*: new data on vegetative and fertile structures, and on its geographic  
757 distribution. Hist. Biol. 27, 345–354.

758 Denayer, J., Webb, G.E., 2015. *Cionodendron* and related lithostrotonid genera from the  
759 Mississippian of eastern Australia: systematics, stratigraphy and evolution. Alcheringa  
760 39, 315–376.

- 761 Dunn, M.T. 2006. A review of permineralized seed fern stems of the upper Paleozoic. J.  
762 Torrey Bot. Soc. 133, 20–32.
- 763 Falcon-Lang, H. J., Galtier, J., 2010. Anatomically-preserved tree-trunks in late Mississippian  
764 (Serpukhovian, late Pendleian-Arnsbergian) braided fluvial channel facies, near  
765 Searston, southwest Newfoundland, Canada. Rev. Palaeobot. Palynol. 160, 154–162.
- 766 Fleming, P.J.G., 1967. Names for Carboniferous and Permian formations. Qd Govt. Mining J.  
767 68, 113–116.
- 768 Galtier, J., 1988. Morphology and phylogenetic relationships of early pteridosperms. *In*: Beck,  
769 C.B. (Ed.) Origin and Evolution of Gymnosperms. Columbia University Press, New  
770 York, pp. 135–176.
- 771 Galtier, J., 2002. *Pitus*, a giant tree of the Early Carboniferous time. *In*: Dernbach, U.,  
772 Tidwell, W.D. (Eds.), Secrets of Petrified Plants. Fascination from Millions of Years.  
773 D'Oro Publ., Heppenheim, Germany, pp. 34–37.
- 774 Galtier, J., Beck, C.B., 1992 *Triichnia*, a new eustelic calamopityacean from the Lower  
775 Carboniferous of France. Palaeontographica 224B, 1–16.
- 776 Galtier, J., Scott, A.C., 1985. Diversification of early ferns. Proc. R. Soc. Edinb. 86, 289–301.
- 777 Galtier, J., Scott, A.C., 1990. On *Eristophyton* and other gymnosperms from the Lower  
778 Carboniferous of Castleton Bay, East Lothian, Scotland. Geobios 23, 5–19.
- 779 Galtier, J., Scott, A.C., 1994. Arborescent gymnosperms from the Visean of East Kirkton,  
780 West Lothian, Scotland. Tran. R. Soc. Edinb. 84, 261–266.
- 781 Galtier, J., Phillips, T.L., 1999. The acetate peel technique. *In*: Jones, T.P., Rowe, N.P. (Eds.),  
782 Fossil Plants and Spores: Modern Techniques. The Geological Society, London, pp. 67–  
783 70.
- 784 Galtier, J., Meyer-Berthaud, B., 2006. The diversification of early arborescent seed ferns. J.  
785 Torrey Bot. Soc. 133, 7–19.

786 Galtier, J., Schneider, J.-L., Grauvogel-Stamm, L., 1998. Arborescent gymnosperms and the  
787 occurrence of *Protopitys* from the Lower Carboniferous of the Vosges, France. Rev.  
788 Palaeobot. Palynol. 99, 203–215.

789 Galtier, J., Feist, R., Talent, J.A., Meyer-Berthaud, B., 2007. New permineralised flora and  
790 trilobites from the mid-Tournaisian (early Carboniferous) Ruxton Formation, Clarke  
791 River Basin, northeastern Australia. Palaeontology 50, 223–243.

792 Gordon, W.T., 1935. The genus *Pitys*, Witham, emend. Trans. R. Soc. Edinb. 58, 279–311.

793 Gould, R.E., 1975. The succession of Australian pre-Tertiary megafossil floras. Bot. Rev. 41,  
794 453–483.

795 Gulbranson, E.L., Montañez, I.P., Schmitz, M.D., Limarino, C.O., Isbell, J.L., Marensi, S.A.,  
796 Crowley, J.L., 2010. High-precision U-Pb calibration of Carboniferous glaciation and  
797 climate history, Paganzo Group, NW Argentina. Geol. Society. Amer. Bull. 122, 1480–  
798 1498.

799 Hass, H., Rowe, N.P., 1999. Thin sections and wafering. In: Jones, T.P., Rowe, N.P. (Eds.),  
800 Fossil Plants and Spores: Modern Techniques. The Geological Society, London, pp. 76–  
801 81.

802 Henderson, E., Falcon-Lang, H.J., 2011. Diversity and ontogeny of *Pitus* tree-trunks in the  
803 early Mississippian rocks of the Isle of Bute, Scotland: The importance of sample size  
804 and quantitative analysis for fossil wood systematics. Rev. Palaeobot. Palynol. 166,  
805 202–212.

806 Henderson, R.A., Davis, B.K., Fanning, C.M., 1998. Stratigraphy, age relationships and  
807 tectonic setting of rift-phase infill in the Drummond Basin, central Queensland. Aust. J.  
808 Earth Sci. 45, 579–595.

809 Hueber, F.M., Galtier, J., 2002. *Symplocopteris wyattii* n. gen. et n. sp.: a zygopterid fern with  
 810 a false trunk from the Tournaisian (Lower Carboniferous) of Queensland, Australia.  
 811 Rev. Palaeobot. Palynol. 119, 241–273.

812 Iannuzzi, R., Pfefferkorn, H.W., 2002. A pre-glacial, warm-temperate floral belt in Gondwana  
 813 (late Visean, Early Carboniferous). PALAIOS 17, 571–590.

814 Jack, R.L., Etheridge, R. Jr., 1892. The geology and palaeontology of Queensland and New  
 815 Guinea. Geol. Surv. Qd Publ. 72, 1–766.

816 Jell, P.A., 2013. Geology of Queensland. Geological Survey of Queensland, Brisbane, 970 pp.

817 Jenkins, T.B.H., Crane, D.T., Mory, A.J., 1993. Conodont biostratigraphy of the Visean Series  
 818 in eastern Australia. Alcheringa 17, 211–283.

819 Johnson, S.E., Henderson, R.A., 1991. Tectonic development of the Drummond Basin,  
 820 eastern Australia: back-arc extension and inversion in a late Paleozoic active margin  
 821 setting. Basin Res. 3, 197–213.

822 Jones, P.J., 1996. Carboniferous (Chart 5). In: Young, G.C., Laurie J.R. (Eds.), Australian  
 823 Phanerozoic Timescales. Oxford University Press, Oxford, U.K., pp. 110–126 + chart 5.

824 Jones, P.J., Metcalfe, I., Engel, B.A., Playford, G., Rigby, J., Turner, S., Webb, G.E., 2000.  
 825 Carboniferous palaeobiogeography in Australasia. In: Wright, A.J., Young, G.C.,  
 826 Talent, J.A., Laurie, J.R. (Eds.), Palaeobiogeography of Australasian Faunas and Floras,  
 827 Association of Australasian Palaeontologists Memoir 23, pp. 259– 286.

828 Kenrick, P., Crane, P.R., 1997. The origin and early diversification of land plants: a cladistic  
 829 study, Smithsonian Institution Press, Washington, DC, 441 pp.

830 Klymiuk, A.A., Harper, C.J, Moore, D.S., Taylor, E.L., Taylor, T.N., Krings, M., 2013.  
 831 Reinvestigating Carboniferous “actinomycetes”: authigenic formation of biomimetic  
 832 carbonates provides insight into early diagenesis of permineralized plants. PALAIOS  
 833 28, 80–92.

834 Konhauser, K.O., 1997. Bacterial iron biomineralization in nature. *FEMS Microbiol. Rev.* 20,  
835 315–326.

836 Krings, M., Harper, C.J., White, J.F., Barthel, M., Heinrichs, J., Taylor, E.L., Taylor, T.N.,  
837 2017. Fungi in a *Psaronius* root mantle from the Rotliegend (Asselian, Lower  
838 Permian/Cisuralian) of Thuringia, Germany. *Rev. Palaeobot. Palynol.* 239, 14–30.

839 Krosch, N.J., Kay, J.R., 1977. Limestone Resources of the Rockhampton region. *Geol. Surv.*  
840 *Qd Rep.* 98, 1–72.

841 Lacey, W.S., 1953. Scottish Lower Carboniferous Plants: *Eristophyton waltoni* sp. nov. and  
842 *Endoxylon zonatum* (Kidston) Scott from Dunbartonshire. *Ann. Bot.* 17, 579–597.

843 Long, A.G., 1979. Observations on the Lower Carboniferous genus *Pitus* Witham. *Trans. R.*  
844 *Soc. Edinb.* 70, 111–127.

845 Maxwell, W.G.H., 1964. The geology of the Yarrol Region. Part 1. Biostratigraphy. *Pap. Dep.*  
846 *Geol. Univ. Qd* 5(9), 1–79.

847 McKelvey, B.C., McPhie, J., 1985. Tamworth Belt. In: Martinez Diaz, C., (general editor),  
848 Wagner, R.H., Winkler Prins, C.F., Granados, L.F. (Eds.), *The Carboniferous of the*  
849 *World II. Australia, Indian subcontinent, South Africa, South America, & North*  
850 *Africa.* Madrid: Instituto Geologico y Minero de Espana: Empresa Nacional Adaro de  
851 *Investigaciones Mineras*, pp. 15–23.

852 McLoughlin, S., Strullu-Derrien, C., 2016. Biota and palaeoenvironment of a high middle-  
853 latitude Late Triassic peat-forming ecosystem from Hopen, Svalbard Archipelago. In:  
854 Kear, B.P., Lindgren, J., Hurum, J.H., Milàn, J., Vajda, V. (Eds.), *Mesozoic Biotas of*  
855 *Scandinavia and its Arctic Territories.* Geological Society of London Special  
856 *Publications* 434, 87–112.

857 Mond, A., 1973. Explanatory Notes on the Dalby 1:250 000 Geological Sheet. Bureau of  
858 Mineral Resources, Australia and Geological Survey of Qld, Brisbane, 24 pp.

859 Morris, N., 1985. The floral succession in eastern Australia. In: Martinez Diaz, C., (general  
 860 editor), Wagner, R.H., Winkler Prins, C.F., Granados, L.F. (Eds.), The Carboniferous  
 861 of the World II. Australia, Indian subcontinent, South Africa, South America, & North  
 862 Africa. Madrid: Instituto Geologico y Minero de Espana: Empresa Nacional Adaro de  
 863 Investigaciones Mineras, pp. 118–123.

864 Murray, C.G., Ferguson, C.L., Flood, P.G., Whitaker, W.G., Korsch, R.J., 1987. Plate tectonic  
 865 model for the Carboniferous evolution of the New England Fold Belt. *Aust. J. Earth*  
 866 *Sci.* 34, 213–236.

867 Murray, C.G., Blake, P.R., Crouch, S.B.S., Hayward, M.A., Robertson, A.D.C., Simpson,  
 868 G.A., 2012. Geology of the Yarrol Province central coastal Queensland. *Queensland*  
 869 *Geol.* 13, 1–675.

870 Olgers, F., 1972. The geology of the Drummond Basin. *Bur. Min. Resour., Geol. Geophys.,*  
 871 *Bull.* 132, 1–78.

872 Playford, G., 1978. Lower Carboniferous spores from the Ducabrook Formation, Drummond  
 873 Basin, Queensland. *Palaeontographica* 167B, 105–160.

874 Playford, G., 1985. Palynology of the Australian Lower Carboniferous: a review. *Compte*  
 875 *Rendu, Dixième Congrès International de Stratigraphie et de Géologie du Carbonifère*  
 876 4, 247–265.

877 Prestianni, C., Rustán, J.J., Balseiro, D., Vaccari, E., Sterren, A.F., Steemans, P., Rubinstein,  
 878 C., Astini, R.A., 2015. Early seed plants from Western Gondwana:  
 879 Paleobiogeographical and ecological implications based on Tournaisian (Lower  
 880 Carboniferous) records from Argentina. *Palaeogeogr. Palaeoclimatol. Palaeoecol.* 417,  
 881 210–219.

882 Pujana, R.R., 2005. Gymnospermous woods from Jejenes Formation, Carboniferous of San  
883 Juan, Argentina: *Abietopitys petriellae* (Brea and Césari) nov. comb. Ameghiniana 42,  
884 725–731.

885 Pujana, R.R., Césari, S.N., 2008. Fossil woods in interglacial sediments from the  
886 Carboniferous Hoyada Verde Formation, San Juan province, Argentina. Palaeontology  
887 51, 163–171.

888 Purdy, D.J., Withnall, I.W., Bultitude, R.J., 2016. Geology, geochronology and geochemistry  
889 of the northeast Drummond Basin Region. Qd Geol. Rec. 2016/01, 1–134.

890 Rasband, W.S., 1997-2016. ImageJ, U. S. National Institutes of Health, Bethesda, Maryland,  
891 USA, <https://imagej.nih.gov/ij/>.

892 Roberts, J., Jones, P.J., Jenkins, T.B.H., 1993. Revised correlations for Carboniferous marine  
893 invertebrate zones of eastern Australia. Alcheringa 17, 353–376.

894 Rößler, R., Philippe, M., van Konijnenburg-van Cittert, J.H.A., McLoughlin, S., Sakala, J.,  
895 Zijlstra, G. & 35 others, 2014. Which name(s) should be used for *Araucaria*-like fossil  
896 wood? – Results of a poll. Taxon 63, 177–184.

897 Sahni, B., 1932. On the genera *Clepsydropsis* and *Cladoxylon* and on a new genus  
898 *Austrocleipsis*. New Phytol. 31, 270–278.

899 Scott, D.H., 1902. On the primary structure of certain Palaeozoic stems with the *Dadoxylon*  
900 type of wood. Trans. R. Soc. Edinb. 40, 331–365.

901 Scott, D.H., 1924. Fossil plants of the *Calamopitys* type, from the Carboniferous rocks of  
902 Scotland. Trans. R. Soc. Edinb. 53, 569–596.

903 Scott, D.H., Jeffrey, E.C., 1914. On fossil plants, showing structure, from the base of the  
904 Waverly Shale of Kentucky. Phil. Trans. R. Soc. Lond. B 205, 315–373.

905 Simpson, G.A., Webb, G.E., Lang, S., 2012. Rockhampton Group (Cr). In: Murray, C.G.,  
906 Blake, P.R., Crouch, S.B.S., Hayward, M.A., Robertson, A.D.C., Simpson, G.A. (Eds.),

907           Geology of the Yarrol Province central coastal Queensland. Queensland Geology 13,  
 908           90–110.

909   Smoot, E.L., Taylor, T.N., 1983. Filamentous microorganisms from the Carboniferous of  
 910           North America. Can. J. Bot. 61, 2251–2256.

911   Strullu-Derrien, C., McLoughlin, S., Philippe, M., Mørk, A., Strullu, D.G., 2012. Arthropod  
 912           interactions with bennettitalean roots in a Triassic permineralized peat from Hopen,  
 913           Svalbard Archipelago (Arctic). Palaeogeog., Palaeoclimatol., Palaeoecol. 348–349, 45–  
 914           58.

915   Taylor, T.N., Taylor, E.L., Krings, M. 2009. Paleobotany: The Biology and Evolution of  
 916           Fossil Plants. Academic Press, Amsterdam, 1230 pp.

917   Thulborn, T., Warren, A., Turner, S., Hamley, T., 1996. Early Carboniferous tetrapods in  
 918           Australia. Nature 381, 777–780.

919   Tidwell, W.D., Herbert, N., 1992. Species of the Cretaceous tree fern *Tempskya* from Utah.  
 920           Int. J. Plant Sci. 153, 513–528.

921   Veevers, J.J., Mollan, R.G., Olgers, F., Kirkegaard, A.G., 1964. The geology of the Emerald  
 922           1:250,000 sheet area, Queensland. Bur. Miner. Resour. Geol. Geophys. Aust. Rep. 68,  
 923           1–71.

924   Walkom, A.B., 1928. Fossil plants from the Upper Palaeozoic rocks of New South Wales.  
 925           Proc. Linn. Soc. NSW 53, 255–269.

926   Walter, M.R., Des Marais, D., Farmer, J.D., Hinman, N.W., 1996. Lithofacies and biofacies  
 927           of mid-Paleozoic thermal spring deposits in the Drummond Basin, Queensland,  
 928           Australia. PALAIOS 11, 497–518.

929   Walter, M.R., McLoughlin, S., Drinnan, A.N., Farmer, J.D., 1998. Palaeontology of Devonian  
 930           thermal spring deposits, Drummond Basin, Australia. Alcheringa 22, 285–314.

- 931 Walton, J., 1957. On *Protopitys* with a description of a fertile specimen *Protopitys scotica* sp.  
 932 nov. from the Calciferous sandstone series of Durbatonshire. Trans. R. Soc. Edinb. 63,  
 933 333–340.
- 934 Warren, A., Turner, S., 2004. The first stem tetrapod from the Lower Carboniferous of  
 935 Gondwana. Palaeontology 47, 151–184.
- 936 Weaver, L., McLoughlin, S., Drinnan, A.N., 1997. Fossil woods from the Upper Permian  
 937 Bainmedart Coal Measures, northern Prince Charles Mountains, East Antarctica. AGSO  
 938 J. Aust. Geol. Geophys. 16, 655–676.
- 939 Webb, G.E., 1990. Lower Carboniferous coral fauna of the Rockhampton Group, east-central  
 940 Queensland. Mem. Assoc. Australas. Palaeontols 10, 1–167.
- 941 Webb, G.E., 2000. The palaeobiogeography of Eastern Australian lower carboniferous corals.  
 942 Hist. Biol. 15, 91–119.
- 943 Webb, G.E., 2002. Latest Devonian and Early Carboniferous reefs: depressed reef building  
 944 after the middle Paleozoic collapse. In: Kiessling, W., Flügel, E., Golonka, J. (Eds.),  
 945 Phanerozoic Reef Patterns. Society for Sedimentary Geology 72, pp. 239–269.
- 946 White, M.E., 1964. 1963 plant fossil collections from Springsure. Bur. Miner. Resour. Geol.  
 947 Geophys. Aust. Rec. 1964/7, 3–17.
- 948 White, M.E., 1969. Plant fossils from the Springsure sheet area. Appendix 3. In: Mollan,  
 949 R.G., Dickins, J.M., Exon, N.F., Kirkegaard, A.G. Geology of the Springsure 1:250 000  
 950 sheet area, Queensland. Bur. Miner. Resour. Geol. Geophys. Aust. Rep. 123. 97–107.
- 951 White, M.E., 1986. The Greening of Gondwana. The 400 Million Year Story of Australia's  
 952 plants. Reed Books, Frenchs Forest, NSW, 256 pp.

**Figure legends**

**Fig. 1.** General geological map of Queensland showing the location of the Drummond and Yarrol basins and the fossil wood localities.

**Fig. 2.** Detail of the geology of the Drummond Basin.

**Fig. 3.** Detail of the geology of the Yarrol Basin.

A. Map showing the location of the basin and the various deposits. The star indicates the fossil wood locality.

B. More detailed map showing location of poorly exposed strata containing fossil wood between the outcrops of the Lion Creek Limestone (coral faunule C) and a younger unnamed limestone (coral faunule D), thus constraining the age to the latest Viséan (modified from Krosch and Kay 1977 and Webb 1990).

**Fig. 4.** Camera lucida drawing of ray outlines on representative tangential sections of wood in specimens DBW2 (A), DBW6 (B), and DBW5 (C) showing ray size and density in the three morphotypes.

**Fig. 5.** Camera lucida drawings of two successive transverse sections of specimen DBW4 showing the compressed pith (P) and numerous vascular traces (arrows) departing from the same level. (A) DBW4-1, (B) DBW4-2; vertical distance between the two sections is 2 mm.

**Fig. 6.** Ray height and width in the three wood morphotypes from the Drummond Basin showing the absence of clearly distinct size groups. Stars: morphotype 1 (DBW2; n=47), triangles: morphotype 2 (DBW6; n=49), squares: morphotype 3 (DBW5; n=50).

979

980 **Fig. 7.** General aspect of a trunk from the Yarrol Basin in cross-section showing the large  
981 parenchymatous pith (P), secondary xylem (x2) and vascular traces (arrows). Drawn from  
982 peel #YB2-s1.

983

984 **Fig. 8.** Camera lucida drawings of details of primary strand distribution and leaf trace  
985 emission in YB1. Scale bars = 1 mm.

986 A. General view of the best preserved part of the pith-secondary xylem boundary showing  
987 numerous peri-medullary primary xylem strands, two departing leaf traces (T1 and T2) and  
988 the location of other traces at a different level of emission ((T)). In the zones facing T1 and  
989 T2, the primary xylem contains several radially aligned protoxylem poles. The zones noted  $\alpha$   
990 and  $\beta$  are interpreted to represent earlier stages of leaf trace production,  $\beta$  being a more  
991 advanced stage than  $\alpha$ . Slides YB1-A0 + YB1-B0.

992 B. Detail of the pair of traces (T1–T2) illustrated in A. Note the radially aligned protoxylem  
993 strands facing the departing traces. Slides YB1-A0.

994

995

- 997 **Plate legends**
- 998 **Plate I. Wood morphotypes from the Drummond Basin.**
- 999 1. Morphotype I in transverse section showing two rays (R). Note a change in tracheid radial  
1000 diameter (arrow). Slide DBW2-CT.
- 1001 2. Morphotype I in tangential longitudinal section with straight tracheids and relatively low  
1002 rays. Slide DBW2-CL.
- 1003 3. Morphotype I in radial longitudinal section showing the araucarian pitting on the tracheid  
1004 walls and araucarioid cross-field pitting (arrows). Slide DBW2-CR (focused stack).
- 1005 4. Morphotype II in transverse section showing multiseriate rays (R). Slide DBW6-CT.
- 1006 5. Morphotype II in tangential longitudinal section, with low to high multiseriate rays. Slide  
1007 DBW6-CL.
- 1008 6. Morphotype II in radial longitudinal section showing the araucarian pitting on the tracheid  
1009 walls. Slide DBW4-CR (focused stack).
- 1010 7. Morphotype III in transverse section with two large rays (R) and a zone of reduced tracheid  
1011 radial diameter (arrow). Slide DBW8-CT.
- 1012 8. Morphotype III in tangential longitudinal section showing very broad rays. Slide DBW5-  
1013 CL.
- 1014 9. Morphotype III in radial longitudinal section showing the araucarian radial pitting of the  
1015 tracheids and the araucarioid cross-field pitting (arrows). Slide DBW8-CR (focused stack).
- 1016 Scale bars: 1, 2, 4, 5, 7, 8 = 100  $\mu\text{m}$ ; 3, 6, 9 = 50  $\mu\text{m}$ .
- 1017
- 1018 **Plate II. Primary vascular structures in specimens DBW4 (1–4) and DBW6 (5–6) from**  
1019 **the Drummond Basin**

- 1020 1. View of the periphery of the pith (P) in DBW4 showing a small conspicuous departing  
1021 vascular trace (arrow) with a more or less endarch maturation. A possible small strand is  
1022 indicated by an arrowhead on the right. Slide DBW4-CT1.
- 1023 2. Zone of the stele in immediate continuity with that illustrated in 1, showing another  
1024 vascular trace (arrow), which is located slightly further from the pith and appears to have a  
1025 more mesarch maturation. A small strand at the pith periphery is indicated by an arrowhead.  
1026 Slide DBW4-CT1.
- 1027 3. and 4. View of another relatively well-preserved area of the pith (P) and innermost  
1028 secondary xylem (X2) showing another conspicuous vascular trace departing (arrow). The  
1029 location of putative small strands of primary xylem is indicated by two arrowheads. Slide  
1030 DBW4-CT1.
- 1031 5. General view of specimen DBW6 in transverse section, with a group of three small  
1032 vascular traces to lateral appendages (t1–t3) visible in the wood. DBW6-CT
- 1033 6. Detail of one of the three traces in 5. DBW6-CT.
- 1034 Scale bars: 1, 2, 3, 4 = 100  $\mu\text{m}$ ; 5 = 1.5 mm; 6 = 250  $\mu\text{m}$ .

1035

1036 **Plate III. Primary vascular structures in specimen DBW9 from the Drummond Basin**

- 1037 1. General view of the part of the specimen with the preserved pith–secondary xylem  
1038 boundary in transverse section showing the parenchymatous pith (P) with cluster of dark cells  
1039 (\*) and a departing vascular trace (arrow). Slide DBW9-A.
- 1040 2. View of the pith in longitudinal section showing the clusters of dark cells (\*). Slide DBW9-  
1041 B.
- 1042 3. Detail of a cluster in the pith showing the thickened walls of the cells. DBW9-A.

4. Pith-secondary xylem boundary in transverse section, showing the apparent lack of immersed primary strands in the pith (P) and the inner wood (X2) with uni- to biseriate rays. Slide DBW9-A.

5. Detail of the departing vascular trace illustrated in 1. Slide DBW9-A.

Scale bars: 1 = 500  $\mu\text{m}$ ; 2, 4, 5 = 250  $\mu\text{m}$ ; 3 = 100  $\mu\text{m}$ ;

**Plate IV. Trunks from the Yarrol Basin (*Ninsaria* gen. nov.): pith and primary xylem strands.**

1. General view of the periphery of the pith (P) and inner wood (X2) in transverse section. A departing leaf trace (T) is visible on the right. Slide YB1-E0.

2. Detail of pith cells with a dark content. Slide YB1-E0.

3. General view of the periphery of the pith in transverse section showing four very small peri-medullary primary xylem strands composed of a few tracheids (yellow arrowheads). Note enlarged rays in the innermost secondary xylem (X2). This region corresponds to the zone between the traces T1 and T2 on Fig. 8. Slide YB1-A0.

4. Detail of the small peri-medullary primary xylem strand indicated by an asterisk on the previous view. Note the endarch maturation. Slide YB1-A0.

5. General view of the periphery of the pith in transverse section showing part of a departing leaf trace (T) and three peri-medullary strands (arrowheads), two small (left arrowheads) and a larger one (right arrowhead). Note the considerable difference in size between the strands and the trace. Slide YB1-E2.

6. Detail of the large peri-medullary primary xylem strand indicated by an asterisk on the previous view. Slide YB1-E2.

Scale bars: 1 = 2 mm; 2 = 50  $\mu\text{m}$ ; 3, 5 = 500  $\mu\text{m}$ ; 4, 6 = 100  $\mu\text{m}$ .

**Plate V. Trunks from the Yarrol Basin (*Ninsaria* gen. nov.): leaf trace production.**

1. Early stage of leaf trace (red arrowhead) production, with a large triangular strand transitioning closer to the pith-secondary xylem boundary. Secondary xylem files are starting to curve. A small strand composed of a few tracheids is visible on one side of the future trace (yellow arrowhead). Peel YB2-s1.

2 and 3. Two examples of a more advanced stage of leaf trace production showing the production of additional protoxylem strands in a radial plane (red arrowheads). Two small strands composed of a few tracheids are present, one on each side of the future trace (yellow arrowheads). 2: Slide YB1-A0, corresponding to trace T2 on fig. 8; 3: Slide YB1-E0.

4. Later stage of leaf departure showing the large departing trace with radially aligned protoxylem strands. Slide YB1-E1.

5–7: details of the primary xylem strands seen in 2, 3, and 4.

Scale bars: 1, 2, 3, 4 = 500  $\mu\text{m}$ ; 5, 6, 7 = 100  $\mu\text{m}$ .

**Plate VI. Trunks from the Yarrol Basin (*Ninsaria* gen. nov.): secondary xylem.**

1. Innermost wood showing enlarged rays at the contact with the pith (P). Slide YB1-E2

2. Typical wood in transverse section showing multiseriate rays (R). Slide YB1-E2.

3. Detail of a zone showing variations in tracheid shape, size, and wall thickness. Slide YB1-E2.

4. General view of the multiseriate rays in tangential section. Slide YB1-H.

5. Detail of 4 showing a biseriate and two triseriate rays. Slide YB1-H.

6. General view in radial longitudinal section showing rays (R) and radial pitting of the tracheids. Slide YB1-I.

7. Detail of tracheid walls in radial longitudinal section showing multiseriate alternate circular pits with an oblique aperture. Slide YB1-H.

1093 8. Detail of cross-field with numerous small crowded pits. Slide YB1-H.

1094 Scale bars: 1, 2, 5, 6 = 100  $\mu\text{m}$ ; 4 = 250  $\mu\text{m}$ ; 7, 8 = 50  $\mu\text{m}$ .

1095

1097 **Table legends**

1098

1099 **Table 1.** Ray anatomy in tangential longitudinal section for the different morphotypes of  
1100 wood from the Drummond Basin. All measurements are for n = 50 rays. DBW9 is not  
1101 included because only the innermost part of its wood is preserved. W: width; H: height.

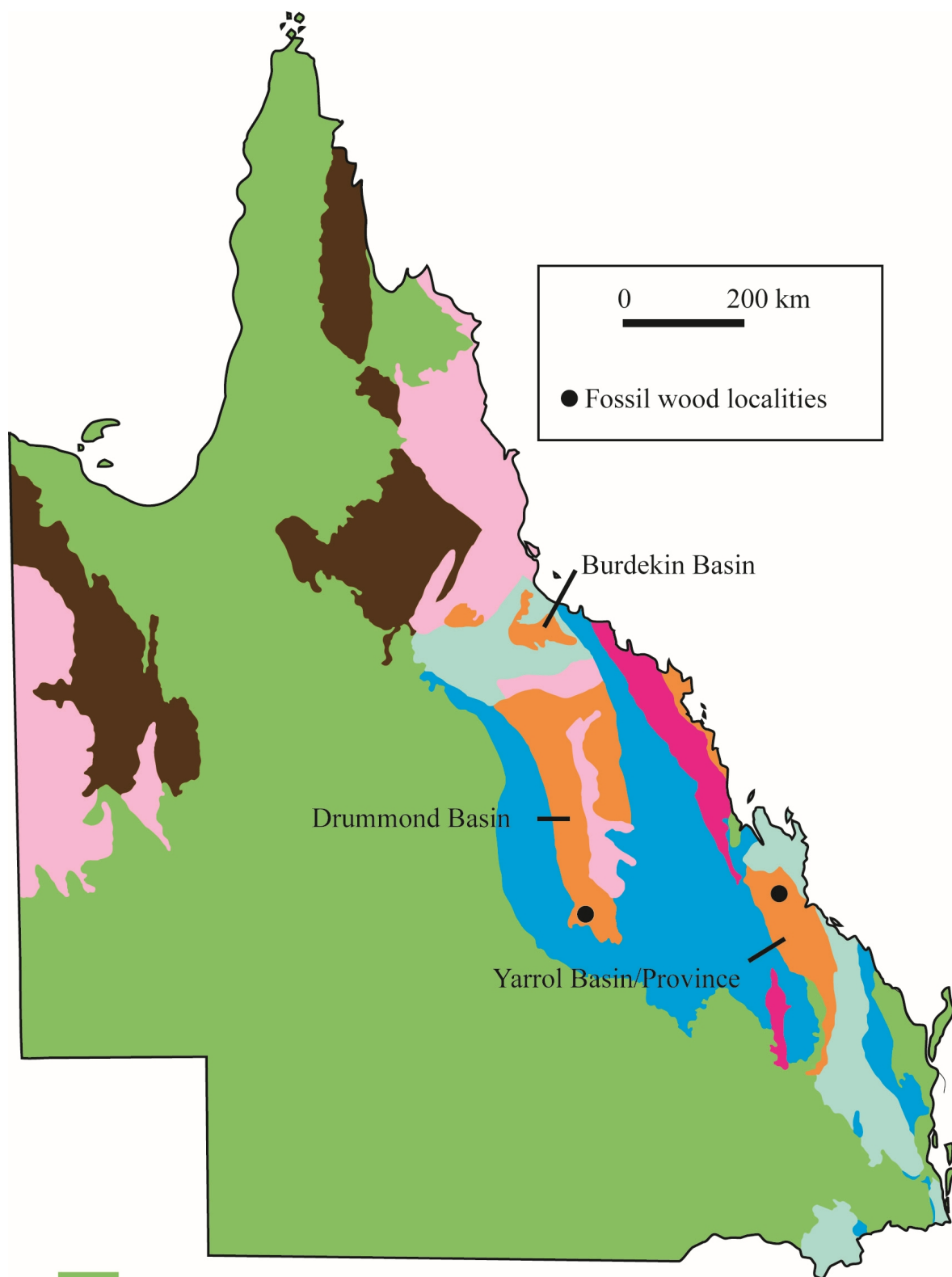
1102

1103 **Table 2.** Comparison of ray size in woods from the Ducabrook Formation and Yarrol Basin  
1104 with other Mississippian arborescent taxa with multiseriate rays from Europe, North Africa,  
1105 North America and Australia.

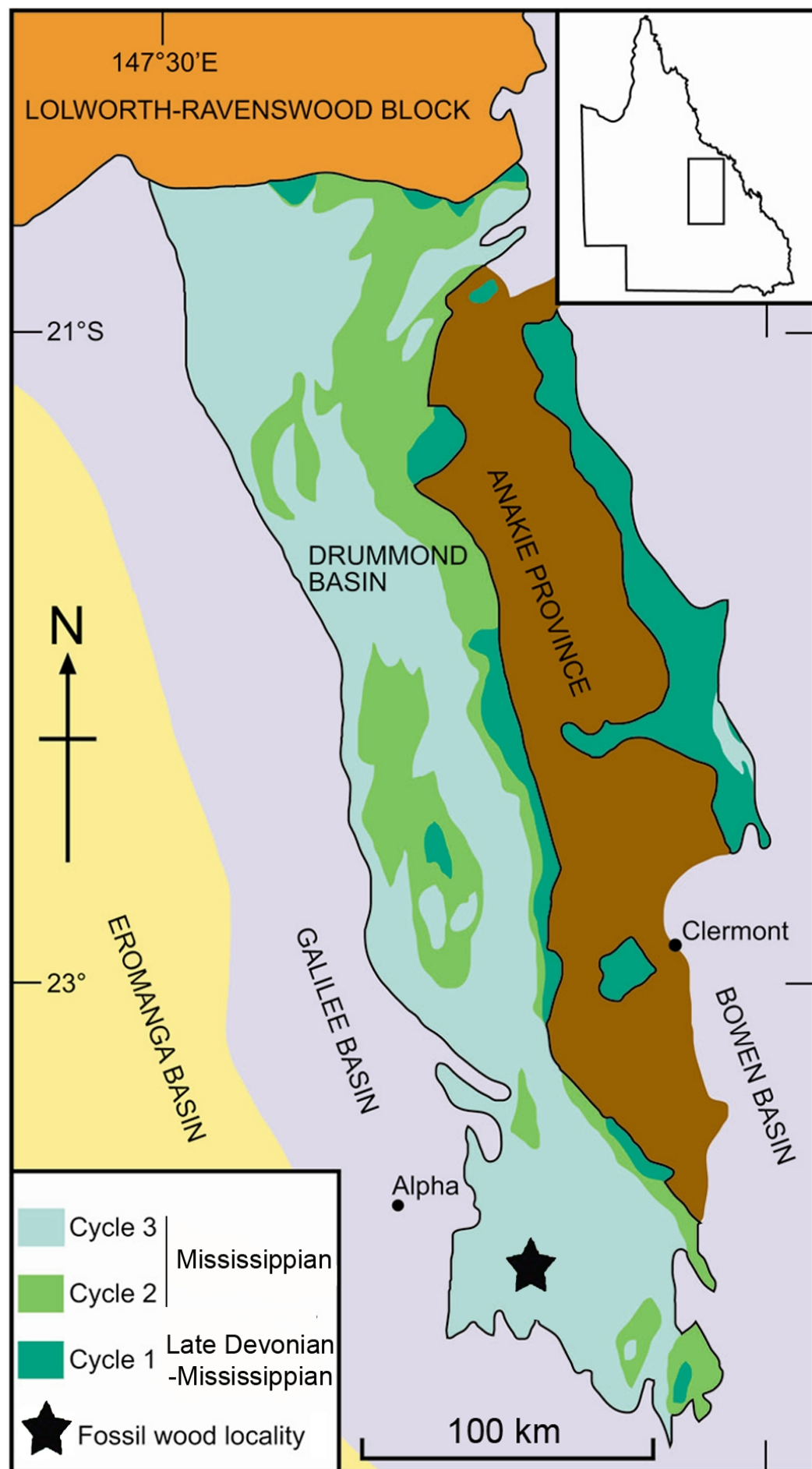
1106

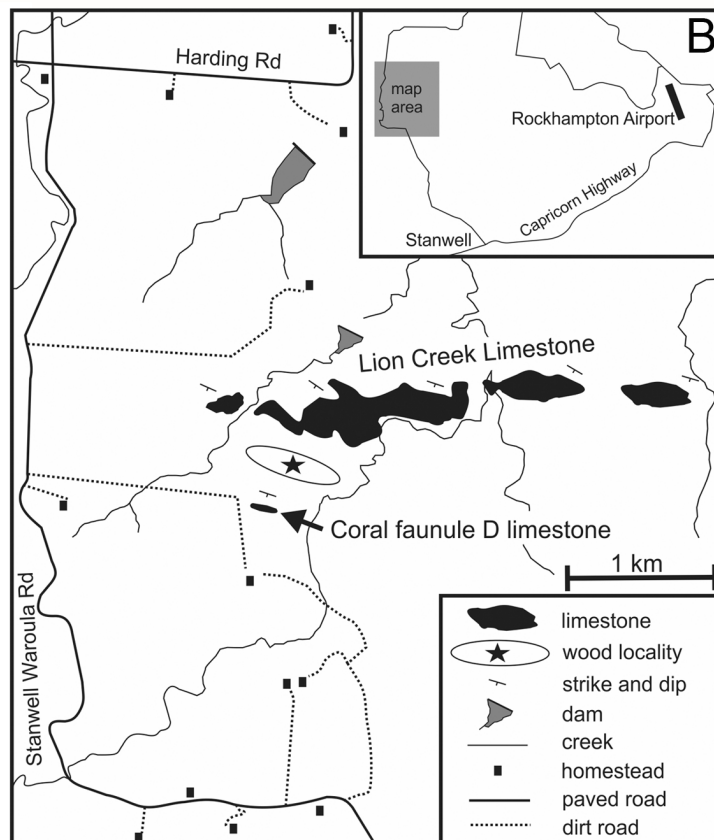
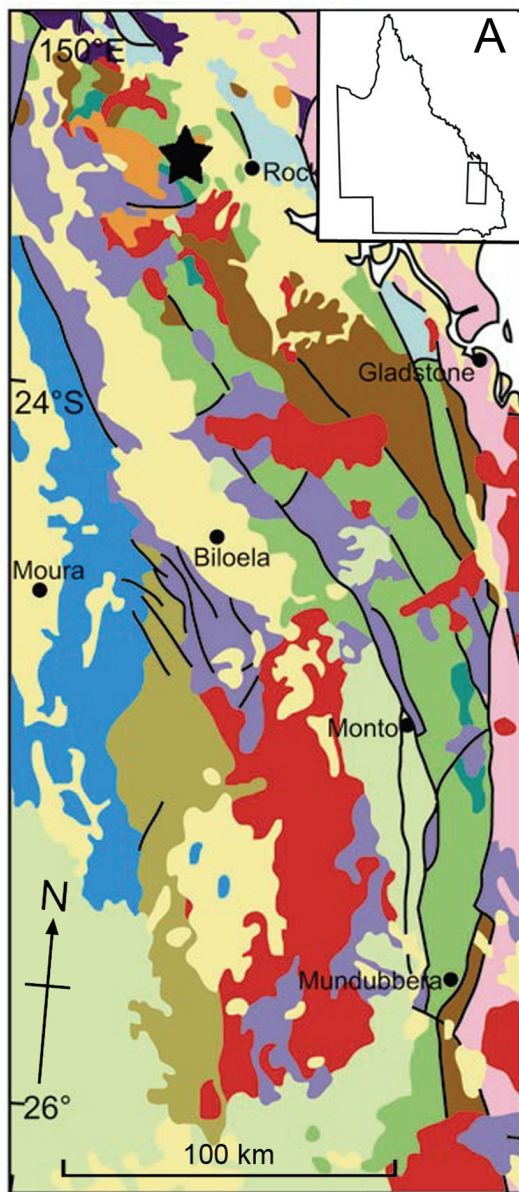
1107

1108



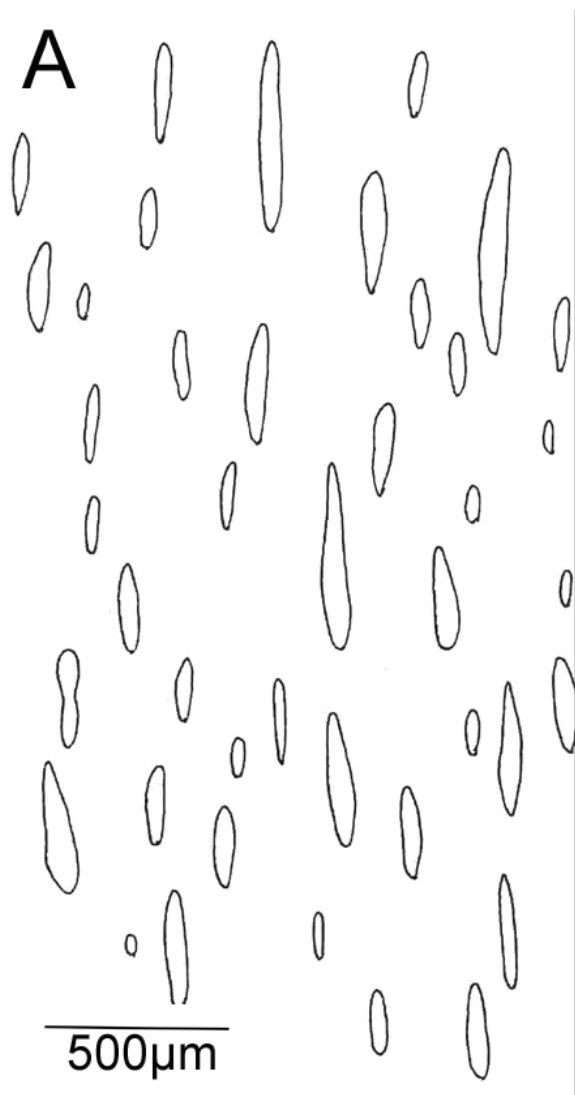
- Jurassic-Cretaceous basins
- Permian-Triassic basins
- Devonian-Carboniferous accretionary prism rocks
- Devonian-Carboniferous forearc and backarc basins
- Mid- to Late Palaeozoic arc-related rocks
- Late Proterozoic to early Palaeozoic
- Palaeoproterozoic to Mesoproterozoic rocks



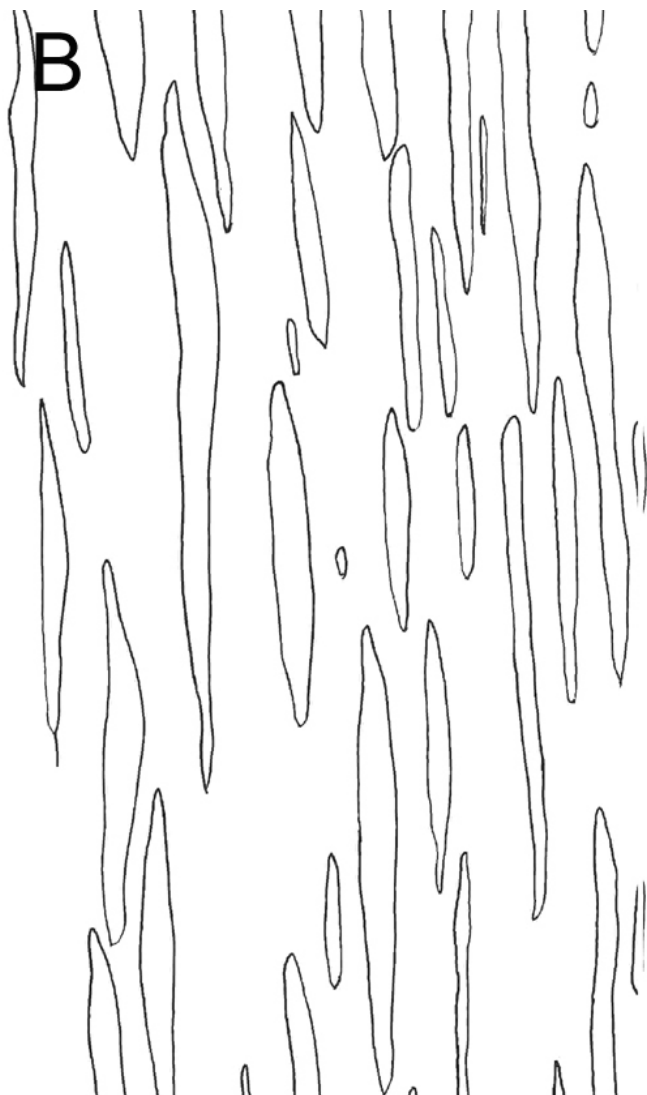


- Cenozoic sedimentary and volcanic rocks
  - Cretaceous sedimentary and volcanic rocks
  - Surat Basin (Jurassic sedimentary rocks)
  - Permian-Triassic intrusives
  - Bowen Basin (Permian sedimentary rocks)
  - Gogango Ovoid Zone (Permian sedimentary rocks)
  - Berziker Graben (Carboniferous-Permian sedimentary rocks)
  - Connors-Auburn Block (Devonian-Carboniferous intrusives)
  - Boiling Creek Group and associated units (Late Carboniferous-earliest Permian sedimentary rocks)
  - Caswell Creek & Rockhampton groups and associated units (Late Devonian-Early Carboniferous sedimentary rocks)
  - Wandilla Province (Devonian-Carboniferous sedimentary and metamorphic rocks)
  - Calliope & Philpott blocks (Devonian-Carboniferous Metamorphic rocks)
  - Marlborough Block (mid-Palaeozoic metamorphic rocks)
- Yarrol Basin

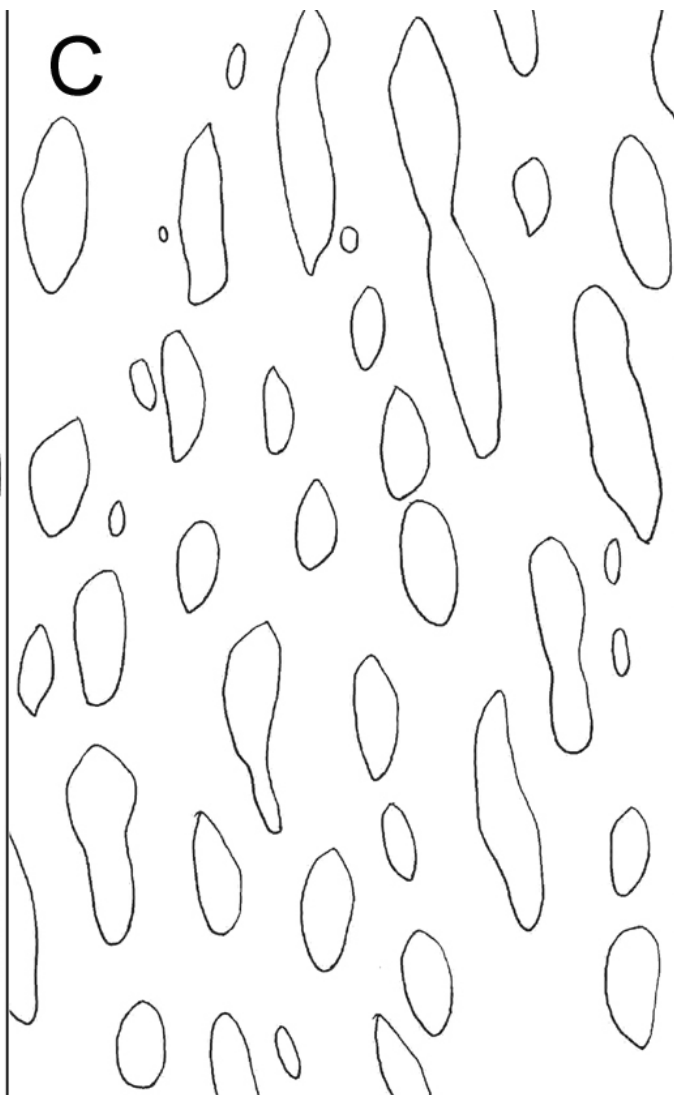
**A**

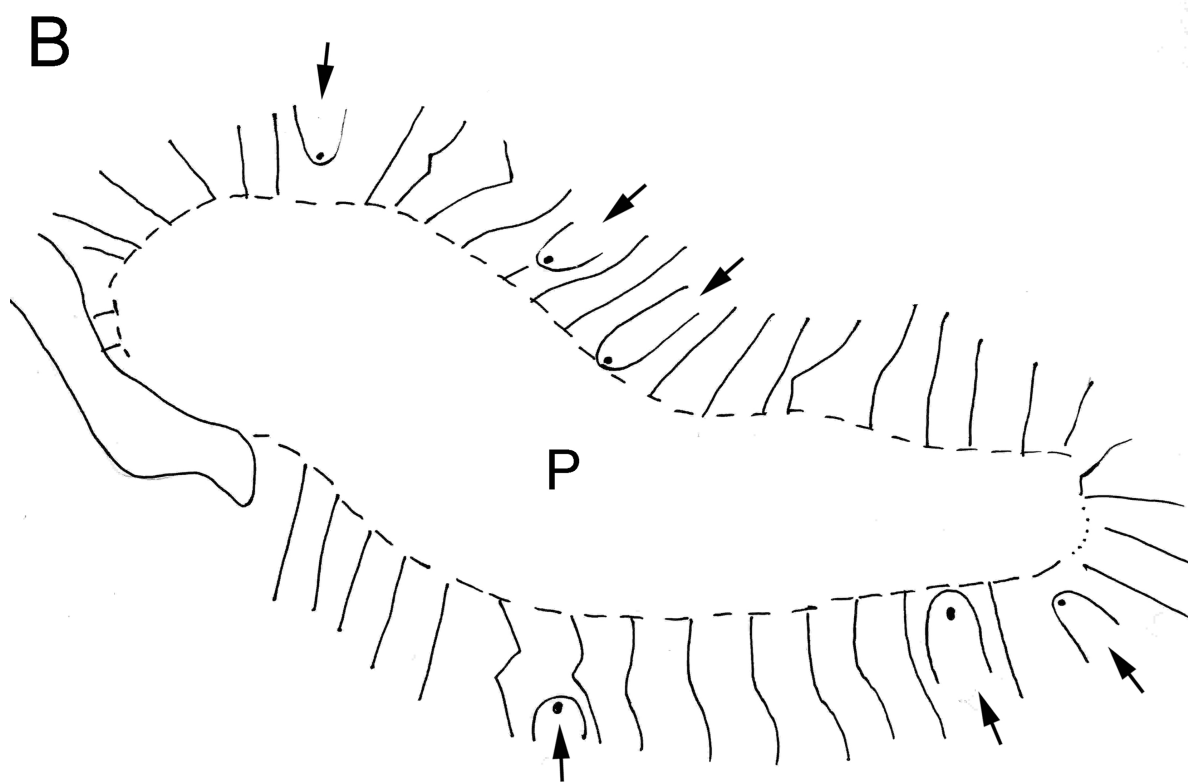
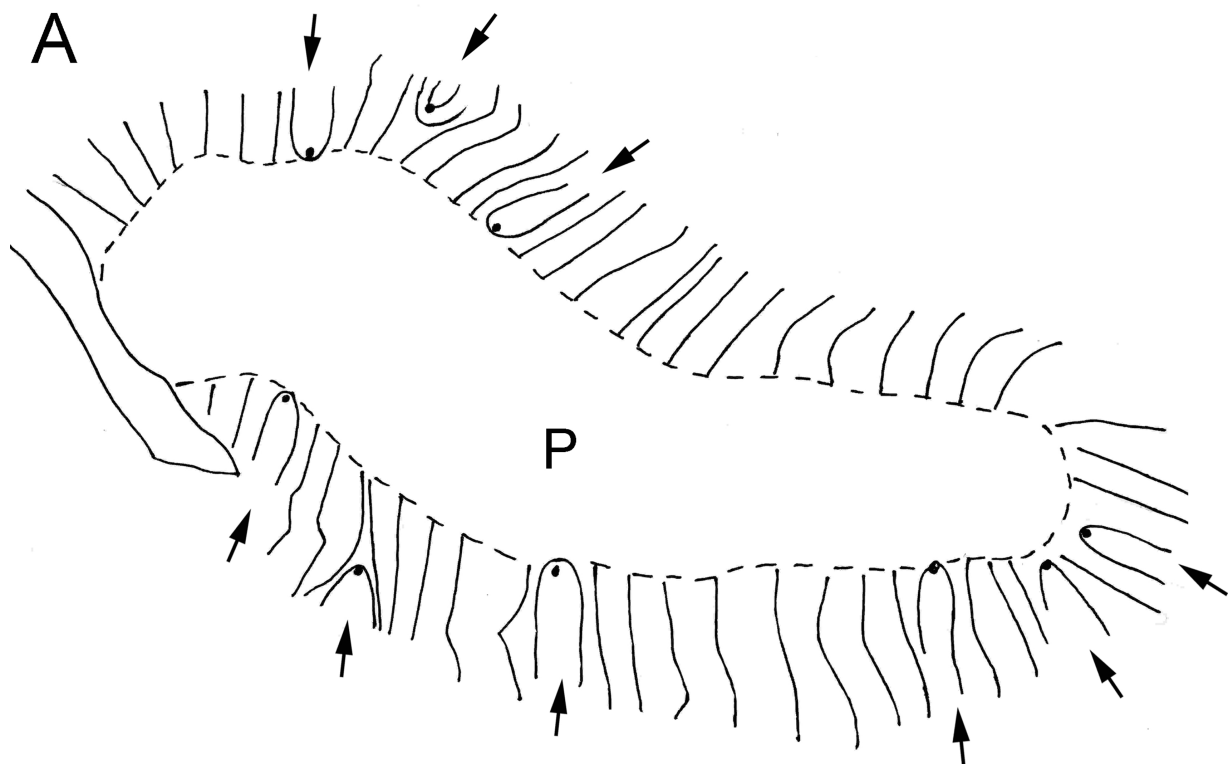


**B**



**C**

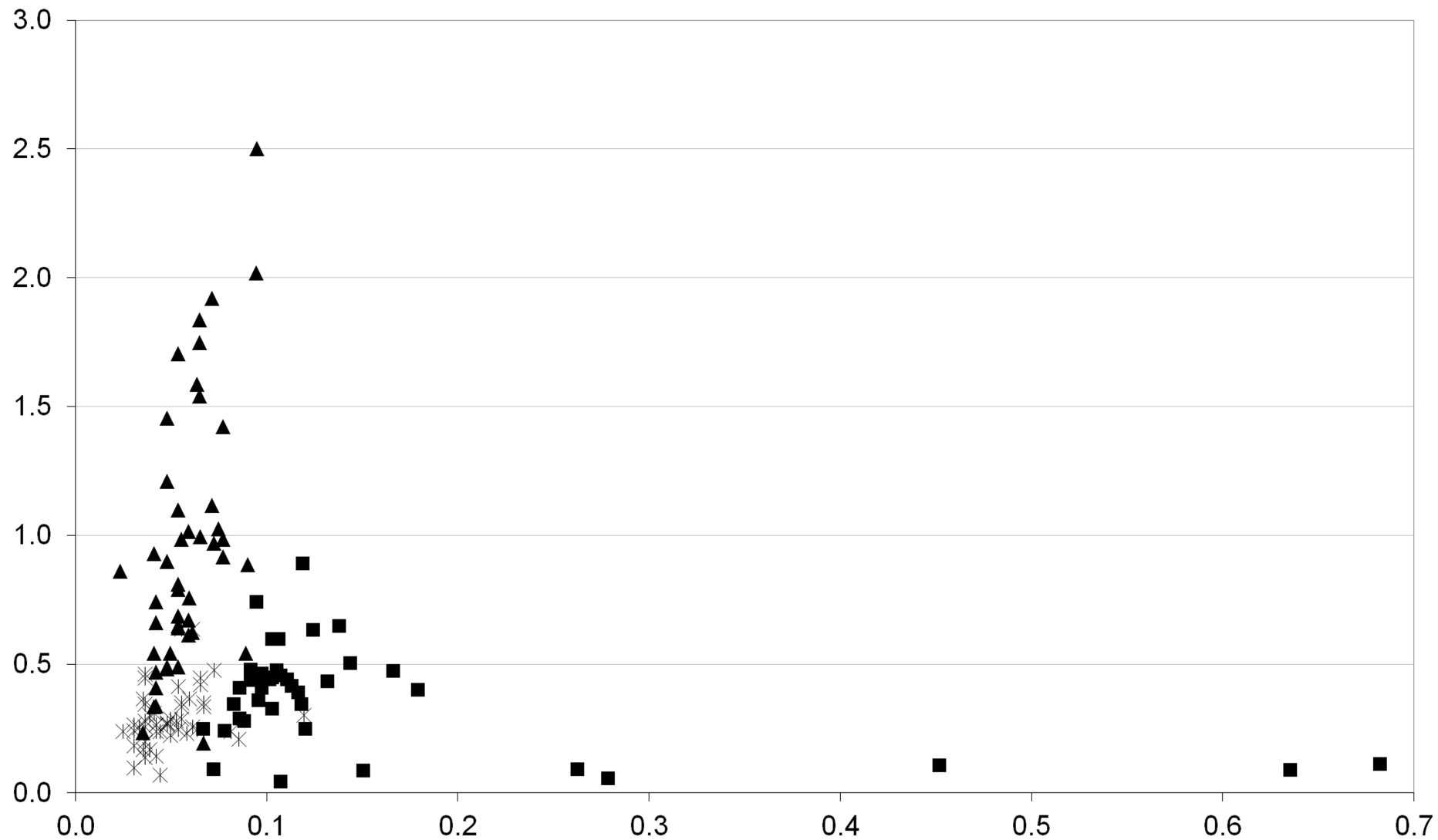


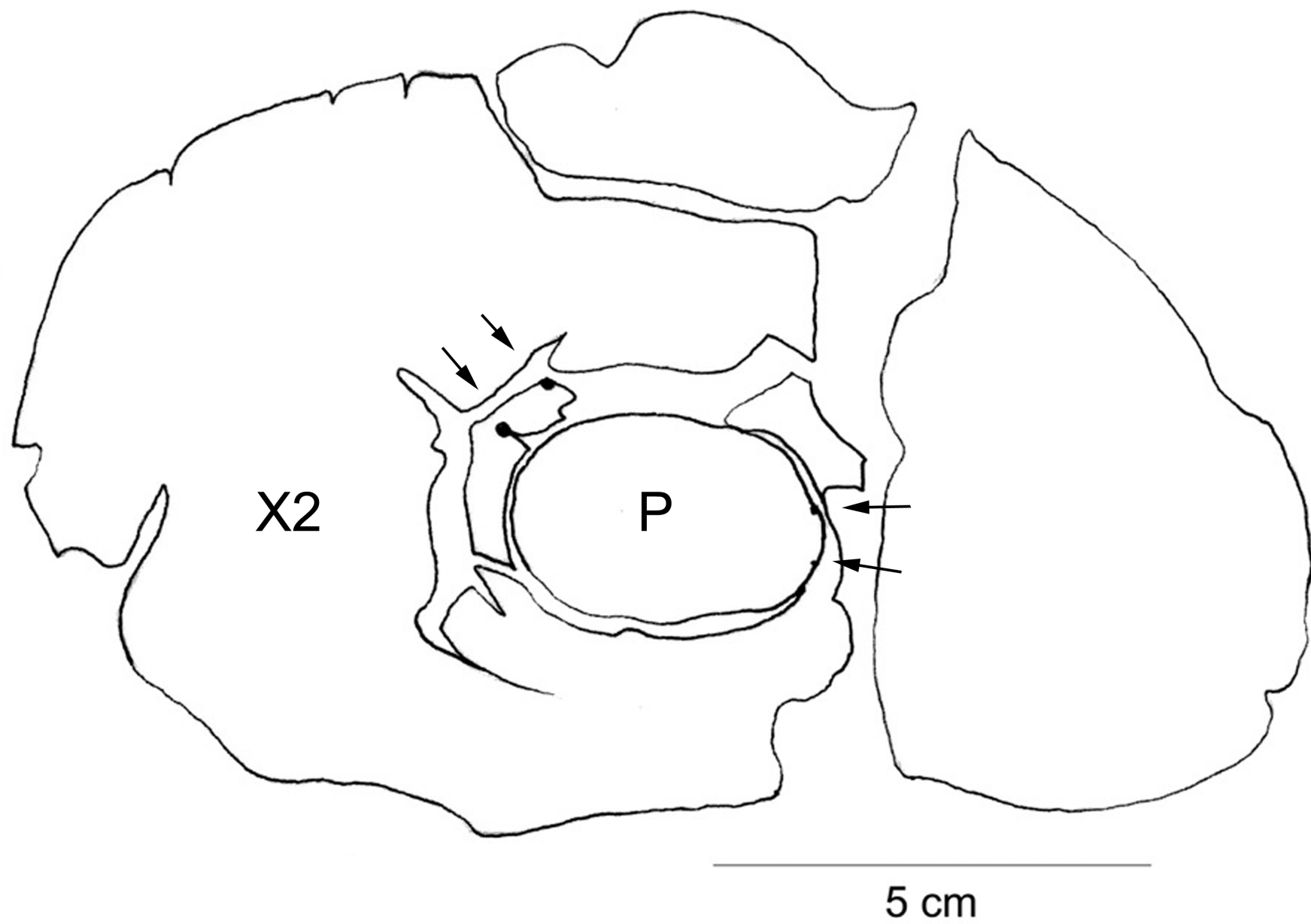


5 mm

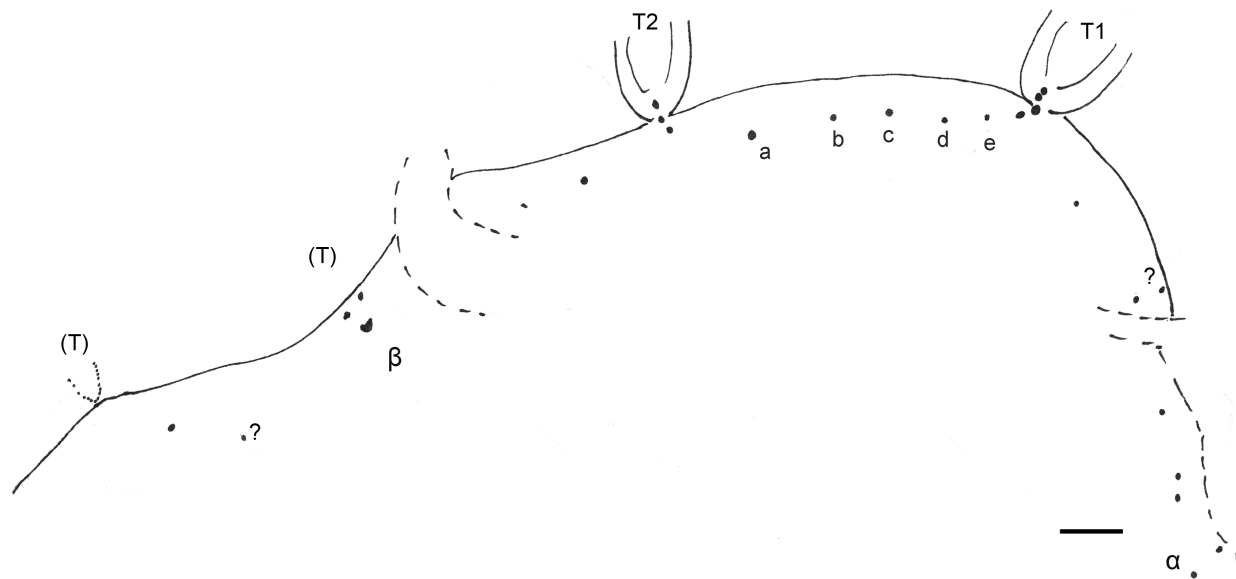
---

Ray height (mm)

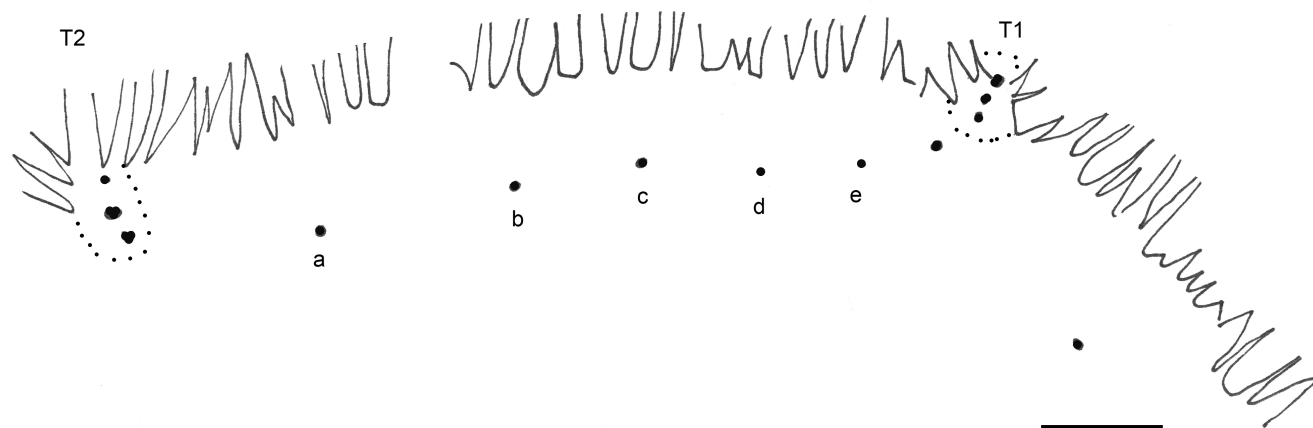


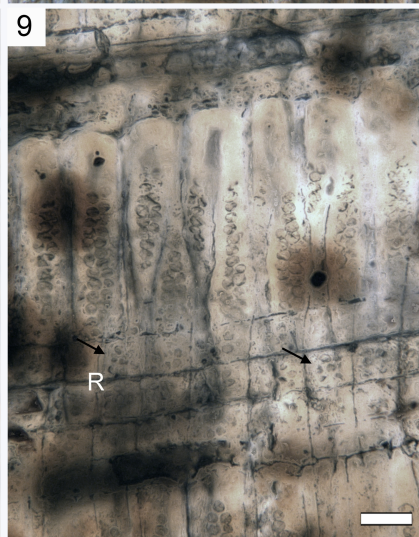
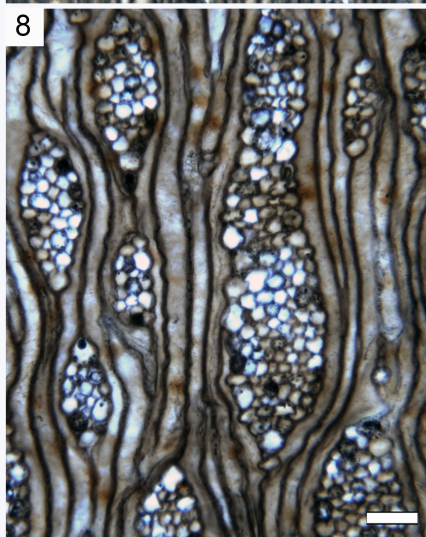
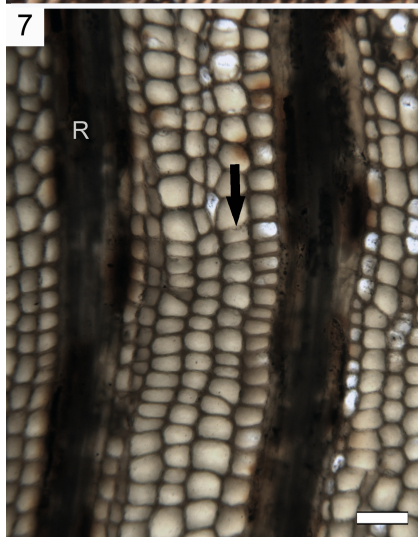
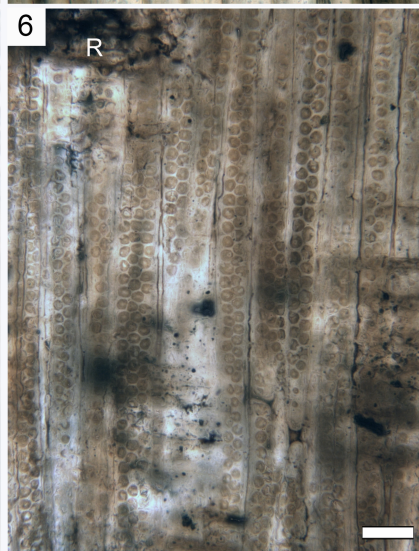
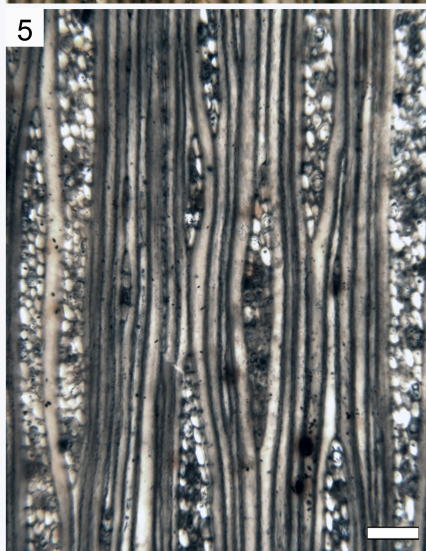
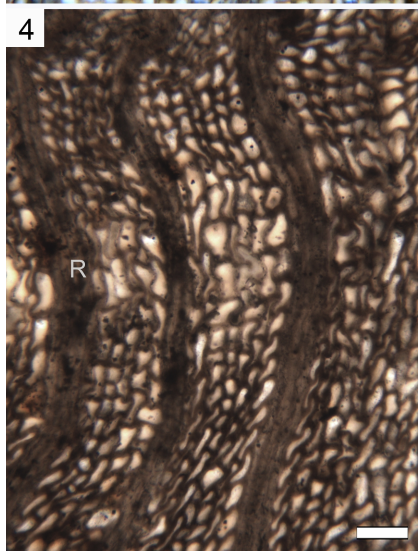
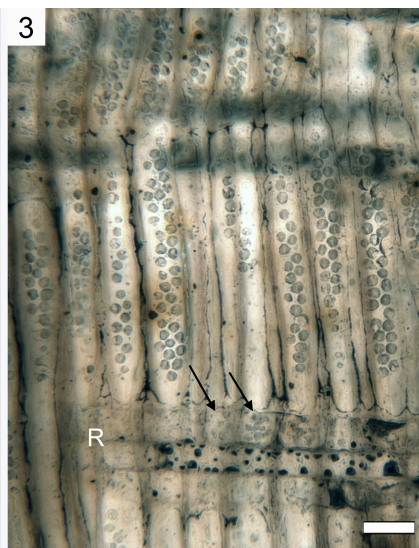


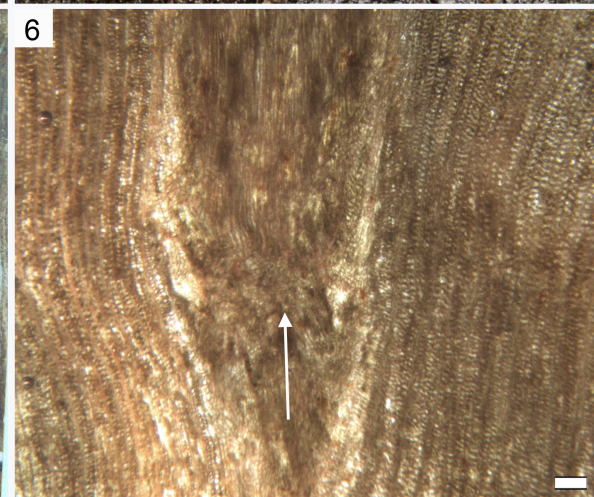
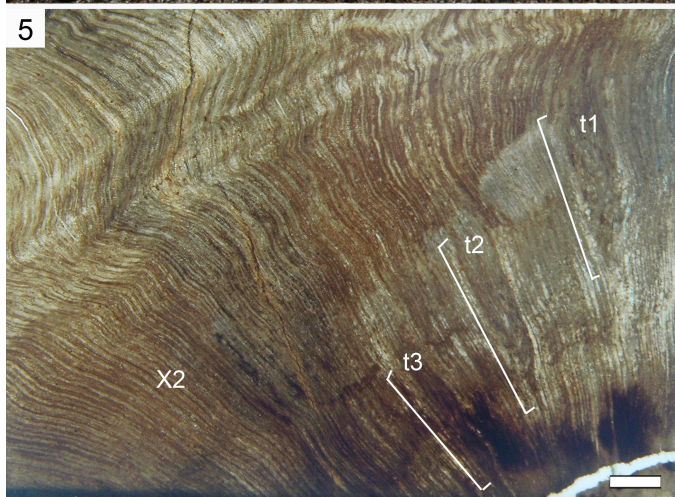
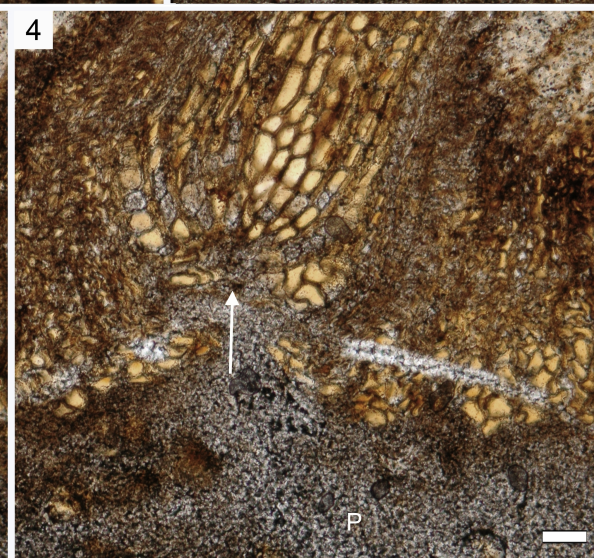
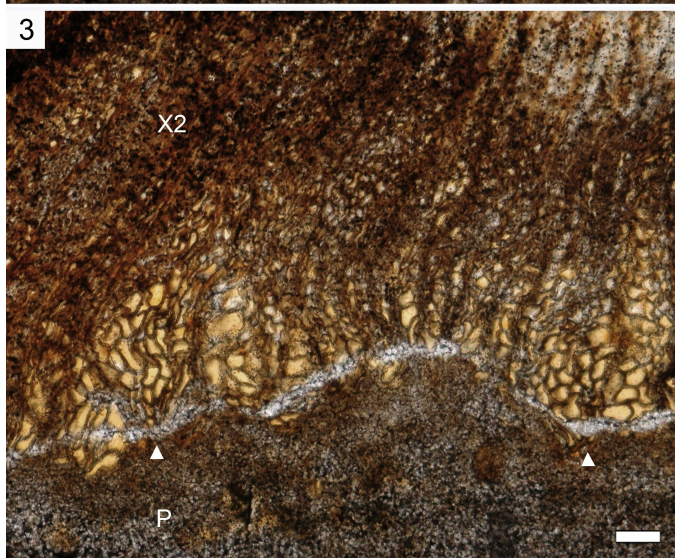
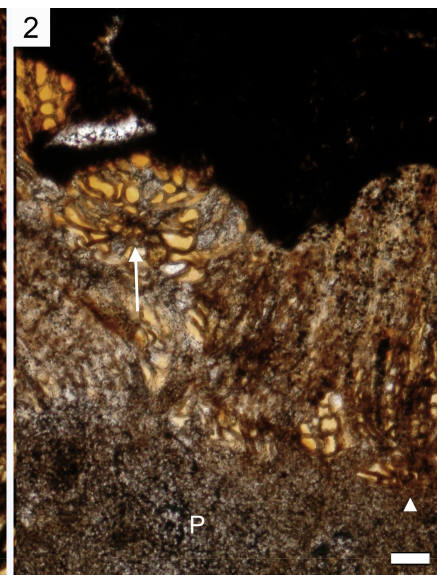
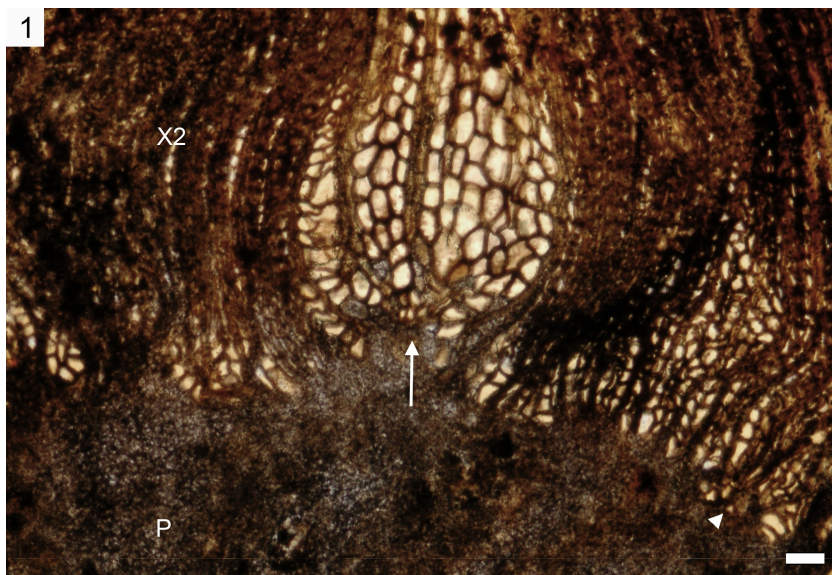
A

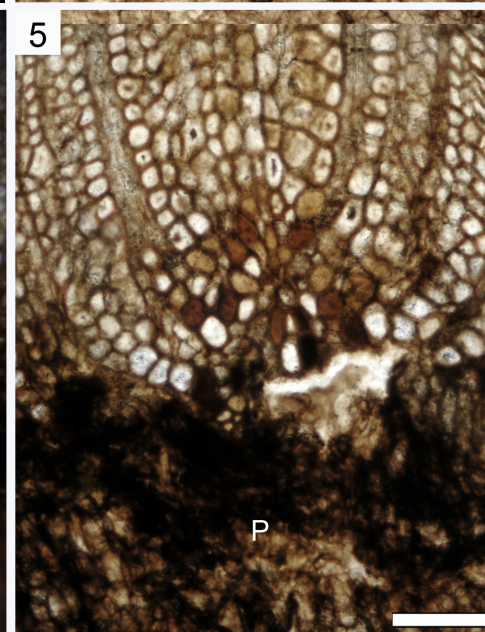
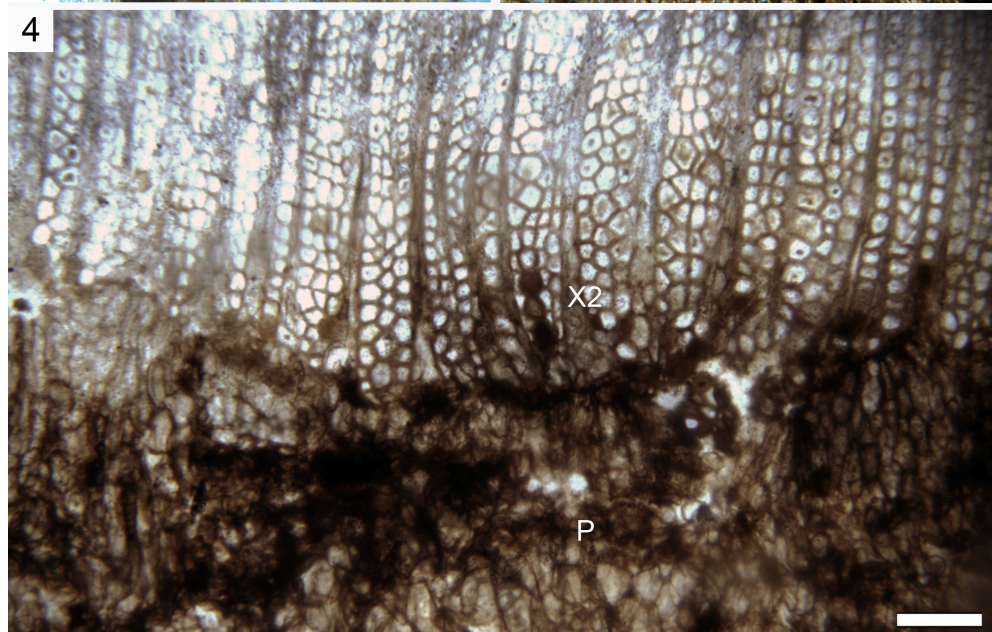
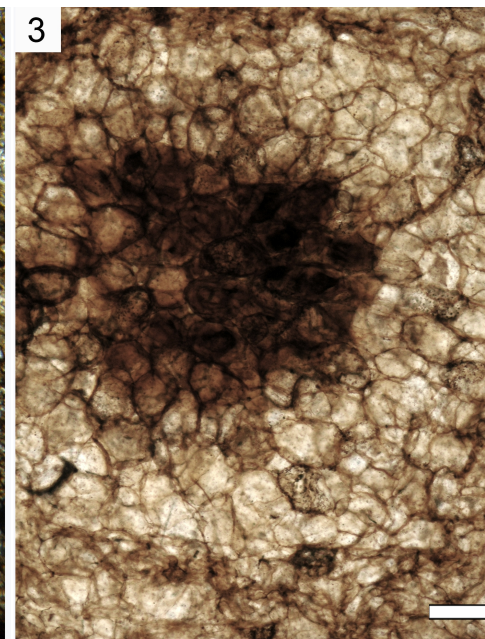
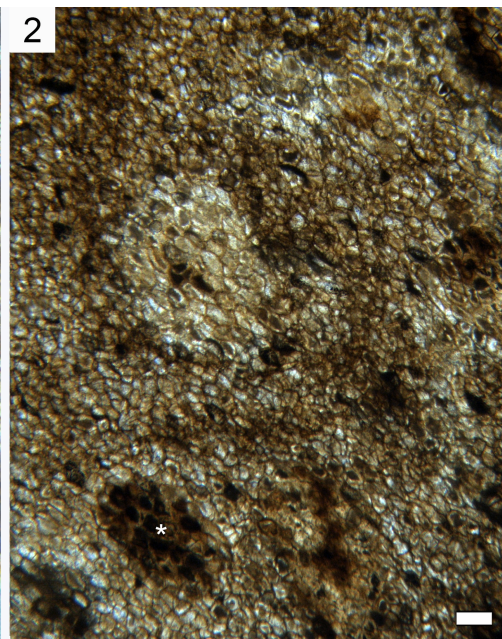
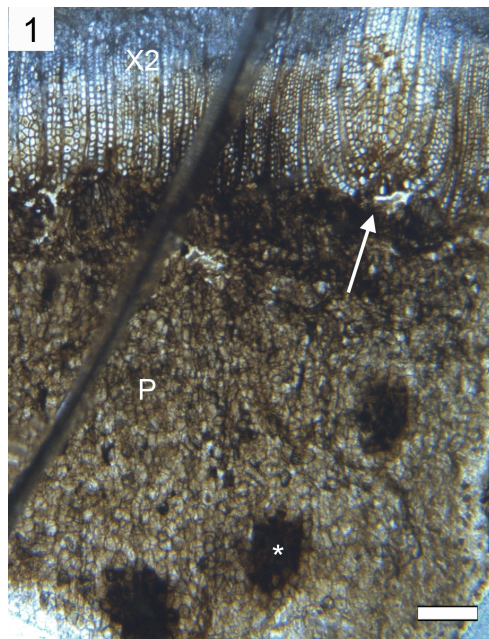


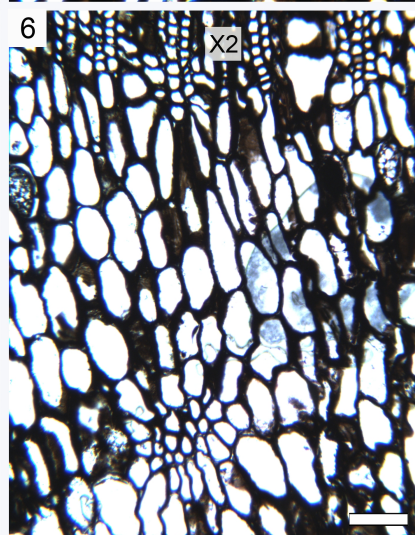
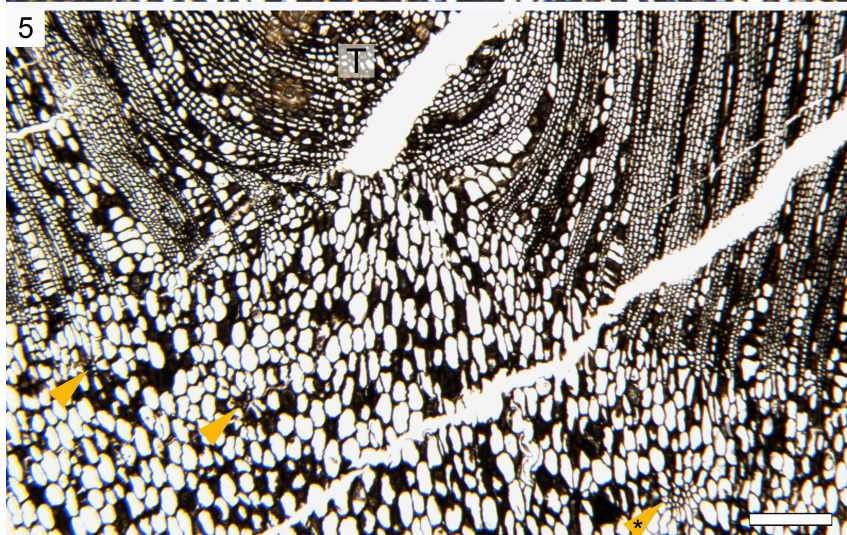
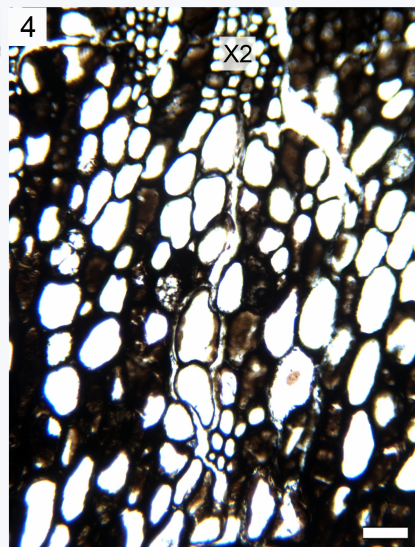
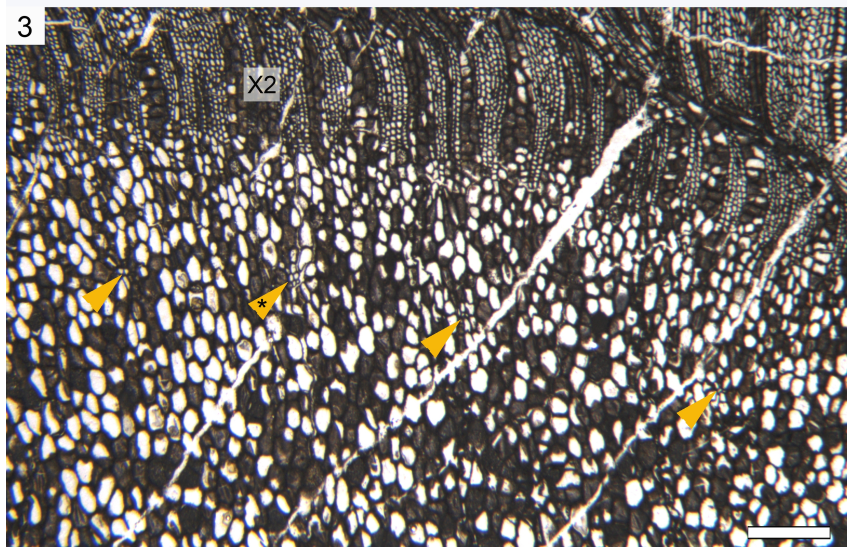
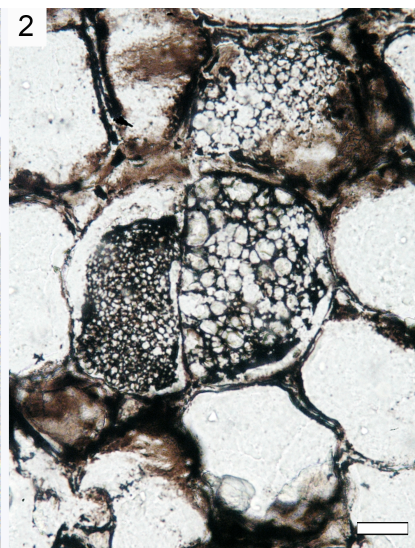
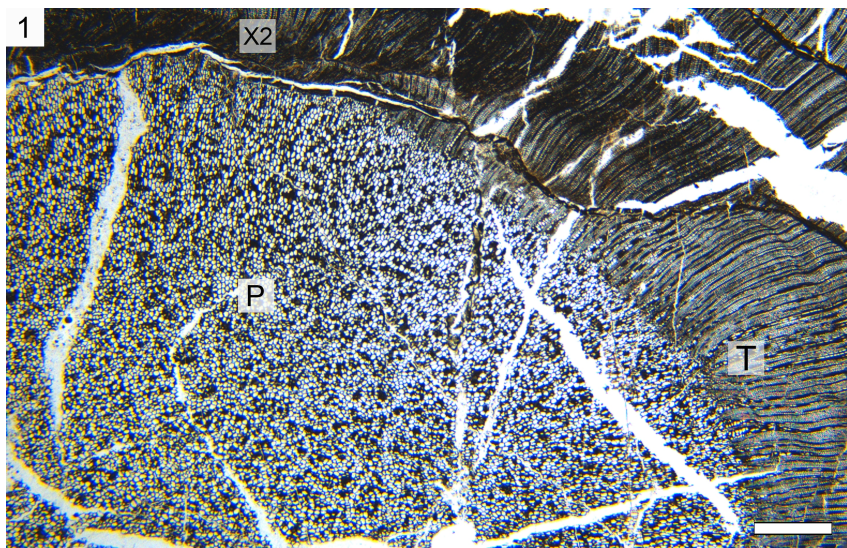
B

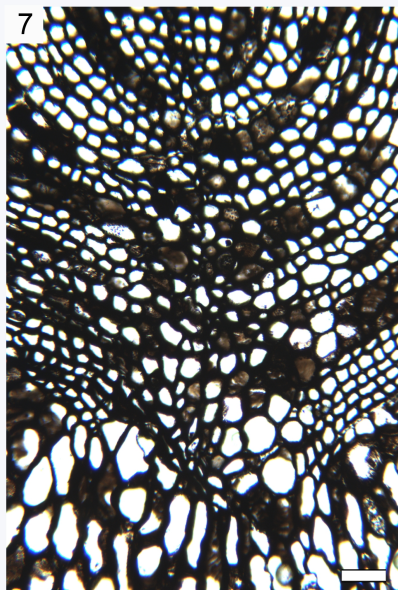
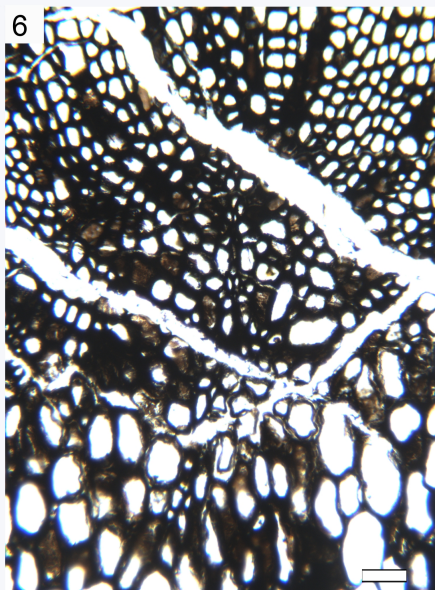
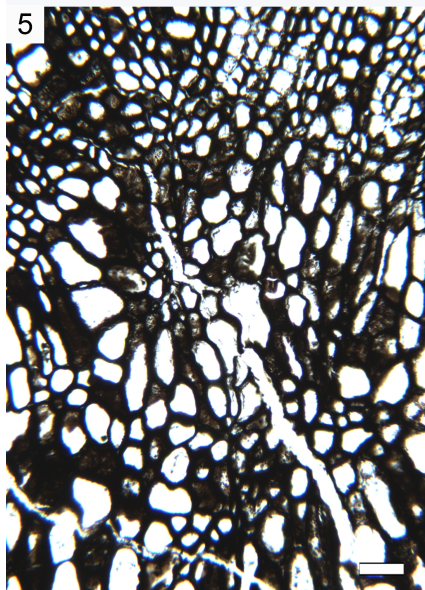
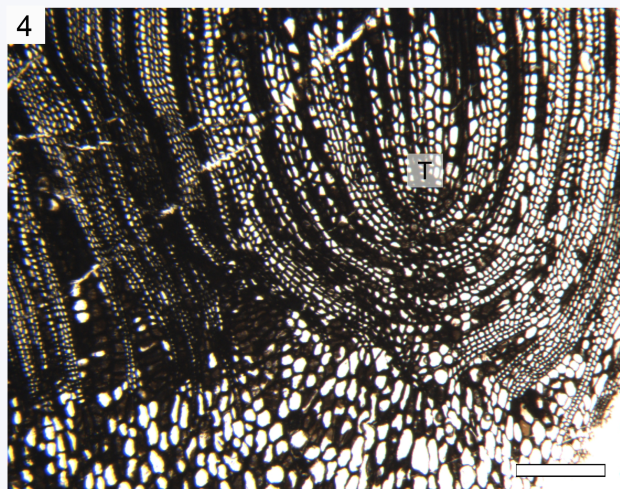
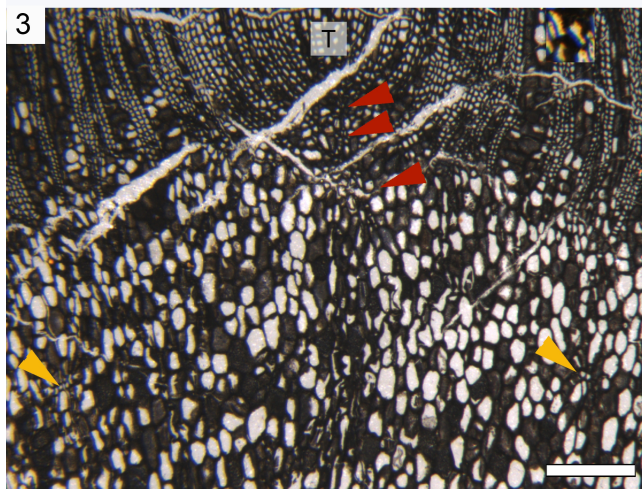
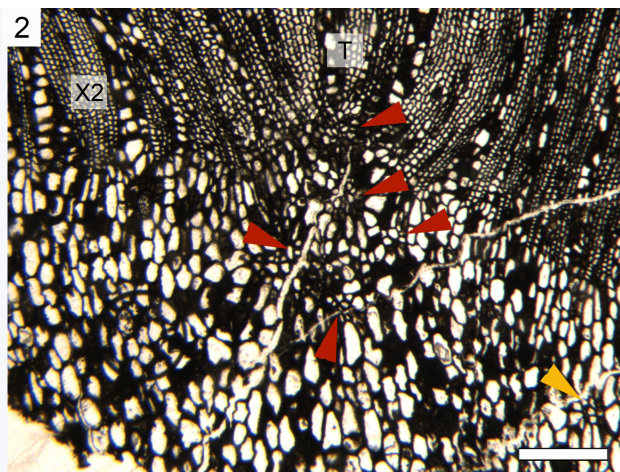
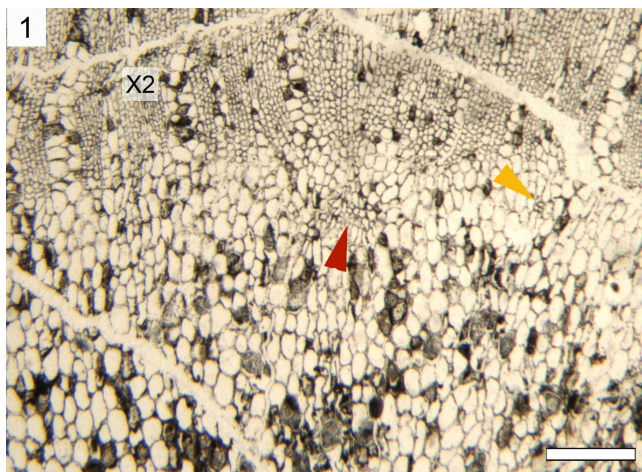


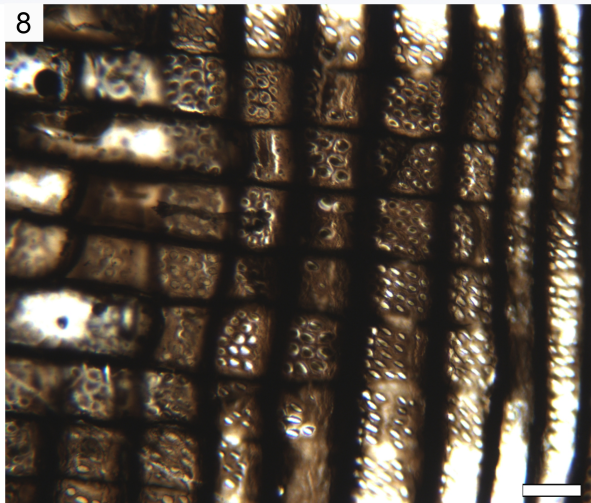
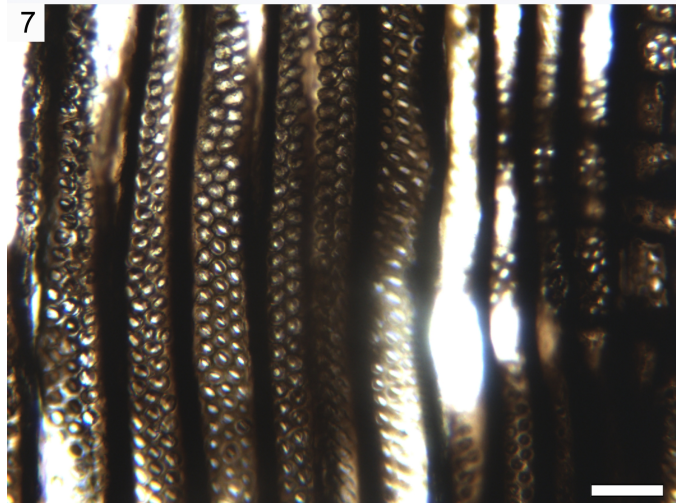
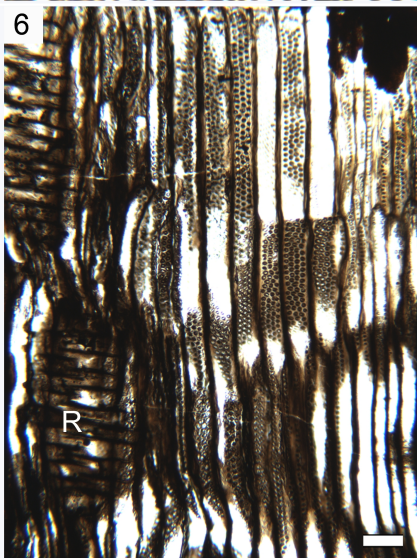
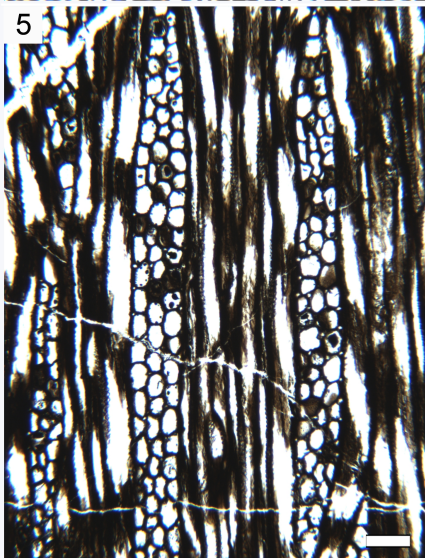
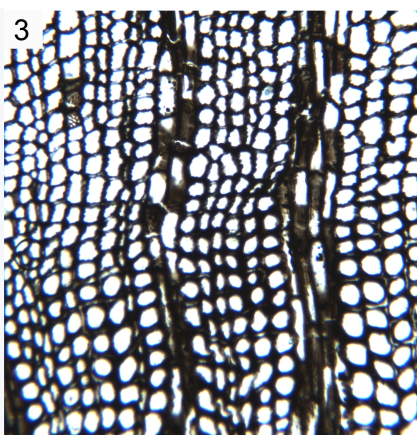
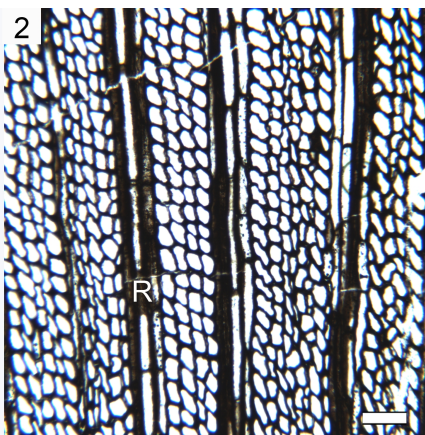
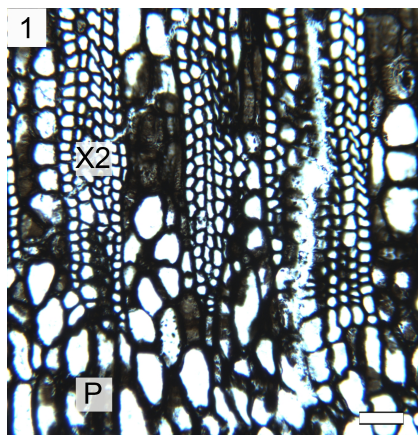












type	Ray width	Ray height	Ray cells (µm)	Ray density	Similar specimens
<b>DBW2</b> Morphotype 1	Cells: 1– <u>1.8</u> –3 Max: 86 µm	Cells: 1– <u>6.2</u> –20 Max: 598 µm	W: 12– <u>22</u> –33 H: 20– <u>31</u> –57 (rectangular)	9 rays/mm <sup>2</sup>	—
<b>DBW5</b> Morphotype 3	Cells: 1– <u>4.5</u> –8 Max: 183 µm	Cells: 1– <u>11</u> –25 Max: 1295 µm	W: 15– <u>27</u> –41 H: 19– <u>29</u> –43 (rounded)	6.5 rays/mm <sup>2</sup>	DBW8
<b>DBW6</b> Morphotype 2	Cells: 1– <u>2.4</u> –4 Max: 116 µm	Cells: 1– <u>21.7</u> –60 Max: 2092 µm	W: 12– <u>18</u> –28 H: 14– <u>31</u> –45 (rectangular)	5 rays/mm <sup>2</sup>	DBW3, DBW4, DBW7, DBW10, DBW11

**Table 1.**

<b>Taxon/morphotype</b>	<b>References</b>	<b>Occurrence</b>	<b>Width (cells)</b>	<b>Height (cells)</b>
DBW2	–	Australia	1– <u>1.8</u> –3	1– <u>6.2</u> –14
DBW5	–	Australia	1– <u>4.5</u> –8	1– <u>11</u> –24
DBW6	–	Australia	1– <u>2.4</u> –4	1– <u>21.7</u> –56 (100)
Yarrol trunk	-	Australia	1– <u>2.7</u> –5	1– <u>14</u> –50
<i>Ahnetia conradii</i>	Decombeix and Galtier, 2017	North Africa	1–2 (5)	1–( <u>10</u> – <u>20</u> )–50
<i>Archaeopitys eastmanii</i>	Scott and Jeffrey, 1914	North America	1–6	1–many (1 mm)
<i>Cauloxylon ambiguum</i>	Cribbs, 1939	North America	1–( <u>3</u> – <u>4</u> )–7	1–( <u>30</u> – <u>50</u> )–92
<i>Dadoxylon ambiguum</i>	Frentzen, 1931 in Galtier et al., 1998.	Europe	1– <u>1.5</u> –3	1–( <u>1</u> – <u>10</u> )–35
<i>Eristophyton waltonii</i>	Lacey, 1953	Europe	1– <u>2</u> –5	1–( <u>5</u> – <u>10</u> )–50
<i>E. fasciculare</i>	Scott, 1902; Galtier and Scott, 1990, 1994.	Europe	1– <u>1.5</u> –3	1– <u>7</u> –22
<i>Faironia difasciculata</i>	Decombeix et al., 2006	Europe	1– <u>1.5</u> –4	1– <u>6.5</u> –28
<i>Megalomyelon myriodesmon</i>	Cribbs, 1940	North America	<u>1</u> –3	1–( <u>30</u> – <u>50</u> )–90
<i>Picnoxylon leptodesmon</i>	Cribbs, 1938	North America	<u>1</u> –3	1–( <u>10</u> – <u>15</u> )–50
<i>Pitus antiqua</i>	Gordon, 1935	Europe	2– <u>3</u> –5	1–70
<i>P. withamii</i>	Gordon, 1935	Europe	1– <u>1.7</u> –4	2– <u>14</u> –78
<i>P. primaeva</i>	Gordon, 1935	Europe	8– <u>10</u> –15	1–60

<i>P. dayi</i>	Gordon, 1935	Europe	4- <u>5</u> -6	1-36
<i>Pitus sussmilchii</i>	Walkom, 1928	Australia	1-4	1-24
MSM11	Decombeix et al., 2011b	Australia	1- <u>2.2</u> -6	1- <u>17.7</u> -50

**Table 2.**